Lappeenranta University of Technology
School of Energy Systems
Degree Program in Environmental Engineering

Aliakbar Joneidi Jafari

ANALYSIS OF HEAT TRANSFER COEFFICIENT IN SILICA NANOFLUIDS WITH WATER AS BASE FLUID UNDER TRANSITIONAL FLOW

Examiners: Professor Risto Soukka
Lic.Sc. (Tech.) Simo Hammo

Supervisors: Professor Tapio Ala-Nissilä
Dr. Ari Seppälä

ACKNOWLEDGEMENT

First and foremost, I most gratefully thank my research examiner and supervisors, Prof. Risto Soukka, Lic.Sc. (Tech.) Simo Hammo, Prof. Tapio Ala-Nissilä and Dr. Ari Seppälä. Without their assistance and dedicated involvement in every step throughout the process, this dissertation would have never been accomplished. I would like to thank you very much for your support and understanding.

A number of colleagues and friends at the Department of Energy in Aalto University deserve special mention for all contributions on experimental and laboratory work they made to my Master's thesis project, Salla Puupponen who guided me with chemical lab matters, undertook DSC measurements and thermal conductivity measurements, Mika Ahlgren who helped me with the modifications in Heat Exchanger and viscometer, Kari Saari who helped with technical matters for heat exchanger, Leena Stenlund who taught me how to work with DLS device and Valtteri Mikkola who helped with the pressure meter calibration.

Lastly and most importantly, I owe my deep gratitude to my supportive father Jamaleddin and mother Monirossadat who raised me and trained me with the perseverance to become an indispensable man.

The author acknowledges the support by the Academy of Finland through its COMP Center of Excellence grant (project no. 251748), and the EXPECTS project within the Aalto Energy Efficiency program for funding this project.

ABSTRACT

Aliakbar Joneidi Jafari

Analysis of heat transfer coefficient in silica nanofluids with water as base fluid under transitional flow

School of Energy Systems

Environmental Energy Technology

2016

Lappeenranta University of Technology

66 pages, 47 figures, 5 tables, 2 appendices

Examiners: Professor Risto Soukka
Lic.Sc. (Tech.) Simo Hammo

Keywords: Nanofluid, Heat transfer coefficient, Silicon dioxide, Transitional flow, Pressure drop

The effect of Reynolds number variation in a vertical double pipe counterflow heat exchanger due to the changes in viscosity can cause the change in flow regime, for instance, when heats up and cools down, it can convert from turbulent to laminar or inversely, that can have significant effect on heat transfer coefficient and pressure drop. Mainly, the range of transition phase has been studied in this study with the investigation of silica nanofluid dispersed in water in three different concentrations. The results have been compared with distilled water sample and showed a remarkable raise in heat transfer coefficient while pressure drop has been increased respectively, as well. Although pumping power has to go up at the same time and it is a drawback, heat transfer efficiency grows for diluted samples. On the other hand, for the most concentrated sample, effect of pressure drop dominates which leads to decline in the overall efficiency.

TABLE OF CONTENTS

TABLE OF FIGURES

TABLE OF TABLES

NOMENCLATURE

Latin letters and symbols

Symbol	Meaning of the symbol	SI Unit
∀	Volume	m^3
A	Area	m^2
c	Centi	-
atm	Atmosphere	Pa
C	Centigrade (celsius)	^oC
c	Specific heat capacity	J/kg.K
cal	Calorie	J
d	Deci	-
D	Diameter	m
d	Diameter	m
d	Difference	-
f	Friction factor	-
G	Thermal conductance	$W/m^2.K$
g	Gram	G
h	Heat transfer coefficient	$W/m^2.K$
hr	Hour	s
HTC	Heat Transfer Coefficient	$W/m^2.K$
HTR	Heat Transfer Rate	W
Hz	Hertz	1/s
J	Joule	J
K	Kelvin	K
k	Kilo	-
k	Thermal conductivity	W/m.K
l	Length for pressure drop	m
L	Length of heat exchanger	m
L	Liter	L
m	Meter	m
m	Milli	-
min	Minute	s
n	Nano	-
Nu	Nusselt Number	-
P	Poise	Pa.s
p	Pressure	Pa
Pr	Prandtl Number	-
r	Radius	m
Ra	Rayleigh Number	-

Re	Reynolds Number	
s	Second	s
T	Temperature	K or ^{o}C
u	Velocity	m/s
V	Volumetric flow	m^3/s
W	Watts	W

Greek letters

Symbol	Meaning of the symbol	SI Unit
α	Thermal diffusivity	m^2/s
Δ	Difference	-
η	Efficiency	-
μ	Dynamic viscosity	Pa.s
π	Pi number	-
ρ	Density	kg/m^3
υ	Kinematic viscosity	m^2/s
Φ	Thermal power	W
φ	Volume fraction	-

Subscripts

Symbol	Meaning of the symbol
i	Inlet
o	Outlet
s	Surface
D	Diameter
h	Hydraulic
rel	Relative
p	In constant pressure

Superscripts

Symbol	Meaning of the symbol
o	Degree
2	Square
3	Cubic

ABBREVIATIONS[1]

AVG	Average
BC	Boundary Condition
BF	Base fluid
cal	Calculated
CCD	Charge-coupled device
cor	Correlation
DB	Dittus Boelter
DLS	Dynamic Light Scattering
DSC	Differential Scanning Calorimetry
EG	Ethylene Glycol
exp	Experimental
FD	Fully Developed
FF	Friction factor
freq	Frequency
G	Gnielinski
Gr	Grashof Number
H	Hausen
IFS	Intensity Fluctuation Spectroscopy
Lam	Laminar
LMTD	Logarithmic Mean Temperature Difference
Max	Maximum
meas	Measured
Min	Minimum
NF	Nanofluid
par	Particle
PCS	Photon Correlation Spectroscopy
PdI	Polydispersity Index
QELS	Quasi-Elastic Light Scattering
RD	Relative Difference
sil	Silica
ST	Sieder and Tate
TEM	Transmission Electron Microscopy
theo	Theoretical
Tran	Transition
Turb	Turbulent
W	Water

[1] These include all the abbreviations and nomenclatures used during the whole project, as well as in Excel documents, so the ones not mentioned in this manuscript have been already used in the calculations

1. INTRODUCTION

New technologies bring new opportunities to the science that will help societies to improve their qualities. One of these qualities is energy efficiency which is a crucial topic because of the limitations in the fossil fuel resources from extraction, implementation and also harms from the emission point of view. Those constraints imposed us to introduce new energy resources such as renewable energies or produce energy from decline in consumption. If we can produce or utilize energies in a way that have more efficiency we can reduce emissions and devote the energy to the more deprived areas, so as a result, more people can benefit from the same consumption.

One of the main processes in energy conversion is to transfer it from a place to another with the aid of cables or pipes, if it is electrical or heating energy, respectively. Heat can be transferred within near or far distances from as small as a microprocessor cooling to as big as a district heating system used to heat up the houses directly from the source of heat generation power plant. In these heat transfer processes we have cycles which are mainly closed loop which means there should be a non-consumable fluid flowing inside the tubes that will carry heating energy from a hot area to a cold area in heating equipment such as heaters and heat pumps or inversely from a cold area to a hot area in cooling equipment such as refrigerators and coolers.

With the above mentioned explanations, one target to increase the efficiency of heating and cooling appliances can be to increase the heat transfer potential in the existing heat exchangers without increasing their size or without adding more tubes. This can be done by changing the fluid properties by two means; one idea is to completely replace the fluid with another fluid with better performance. While, the other idea which uses the technology developed in a few decades ago is to add some very small scale solid particles to the fluid to make a suspension. Those particles are in the range from 1-100 nm so this mixture is called nanofluid.

The usage of nanotechnology can return to 9^{th} century for pottery in Mesopotamia. In the modern world, nanofluid appliance can be traced back to 1873 when Maxwell had the revolutionary idea to add small particles to a fluid to increase the thermal conductivity of a heat transfer fluid (K R et al., 2014).

Basically, the nanoparticles are metals or metal oxides as well as non metallic oxides which have larger conductivity. These extremely small particles have haphazard movements in the fluid called Brownian motion. This helps fluid to have more uniform temperature with the raise in the heat transfer in the fluid itself because of those nanoparticles and Brownian motion. These nanofluids have proven to have better heat transfer characteristics without changing the size and shape of heat exchanger. While, the better performances of nanofluids, one should consider some points such as augmentation in the pumping power due to the increase in viscosity or agglomeration of the nanoparticles or sedimentation that is not appropriate to occur. Hence, there should be an optimal limit for the concentration and size of nanoparticles to have the best and acceptable performance.

The first literature survey was to find articles on Ethylene Glycol as a base fluid but throughout the project it was decided to use the silica nanoparticles already dispersed in water as the base fluid. Therefore, initially some information about previous research done on EG will be presented and then will be shifted to the articles written for water as base fluid and in laminar to turbulent region based on the previous research made on ethylene glycol based nanofluids in different types of flows, laminar, transition and turbulent flows.

The ethylene glycol-based titania nanofluids and water-based nano-diamond nanofluids showed no significant enhancement in heat transfer. (Ding et al., 2007)

Among the mixtures they studied, the Ethylene Glycol–Al2O3 nanofluid indicates better heat transfer qualities than water–Al2O3; it is also the one that has contained unfavorable effects on the wall shear stress. For a tube flow case study, as far as the flow Reynolds number increases, the heat transfer improvement augments. (Maïga et al., 2005)

Multi walled carbon nano tube seems to be an appropriate nominee to enhance the convective heat transfer coefficient for the water-ethylene glycol mixture; on the other hand, researchers did not take into account the effect of pressure loss and increase in pumping power which is remarkable in the nanofluids with nanotube particles. (Kumaresan et al., 2013)

High convective heat transfer improvement of nanofluid mixtures that are used as coolants in laminar flows has been reported. (Xie, Li and Yu, 2010)

Heat transfer behaviors of the nanofluids were quite dependent on various factors like the average size, species of the suspended nanoparticles, volume fraction and the flow conditions. Nanofluids containing alumina, zinc oxide, titanium dioxide, and magnesium oxide were made ready with a mixture of 45 vol. % ethylene glycol and 55 vol. % distilled water as base fluid (except titanium dioxide the others depicted better enhancement of heat transfer coefficient) with the maximum improvement up to 252% at a laminar Reynolds number of 1000 for magnesium oxide nanofluids, however, the effect of pressure drop is not considered. (Guo et al., 2010)

As one can notice, there are plenty of articles that reported heat transfer enhancement, however, they neglected the effect of pumping power. Then the literature survey was done for the range of Reynolds number from turbulent flow to laminar region, as transition flow.

"The convective heat transfer coefficient of nanofluids has the highest value at the entrance, but decreases with axial distance and reaches a constant value in the fully developed region. The entrance length depends on the properties and behavior of nanofluids. For a given nanofluid, the entrance length at low flow rates, e.g. laminar flow for Newtonian fluids, is longer than that at high flow rates, e.g. turbulent flow for Newtonian fluids." (Ding et al., 2007)

The deterioration of ethylene glycol-based titania nanofluids is very interesting. It is believed to be related with the high viscosity of the base liquid. (in low Reynolds) There seems to be a correlation between the rheological behavior and convective heat transfer behavior. For instance, for water-based carbon nanotube nanofluids, an extreme rise in the convective heat transfer coefficient happens at a flow rate where shear viscosity is almost near to the lowest. However, from our team's experience, working with titania nanofluids could cause clogging of pipes in some experiments.

In transitional flow, the flow continuously oscillates between laminar and turbulent regimes and inversely. Based on what Reynolds found, transition flow happens in the range of Reynolds number 2000-13000 in which the lowest Reynolds number occurs in the rough entry. However, if one can have a very smooth pipe and keep the pipe without vibration and flow without disturbance, laminar flow can be sustained in higher Reynolds numbers even up to 100,000, the main recognition for a flow to be laminar or turbulent is to track the trace of an ink into a fluid to see its path is linear and smooth or not.

It was needed to gather data and literature that could be applicable to the setup. So based on the previous research which was done on this setup in the horizontal heat exchanger and in turbulent flow, it was decided to use laminar and transition flow in the vertical heat exchanger.

So based on the recommendations, looking for different articles was reasonable to use nanofluids in heat exchangers with laminar and turbulent flow (preferably in the vertical mode) which had Ethylene Glycol partially or totally as the base fluid. Then, because of the unavailability of nanoparticles with the small size to be dispersed in Ethylene Glycol as base fluid, water as the base fluid was chosen. Frequent amount of the articles did not take into account the effect of pressure drop in the pipes, which mostly, neglected pressure drop measurements. So, the literature was written based on the mentioned criteria and following:

- Authors
- Base fluids
- Nanoparticles' material, size and concentration
- Flow arrangements such as flow geometry, horizontal/vertical mode, nanofluid cooling/heating method
- Preparation such as usage of ph adjustment or surfactants, mixing/sonication
- Particle characterization which includes the method used to measure particle size distribution, measurement of distribution from powder or suspension, probability of agglomeration, clusterization or sedimentation
- Methods for evaluation of thermal properties such as thermal conductivity, viscosity, specific heat and density.
- Range of measured Re number and temperature variation
- Results based upon changes in heat transfer coefficient or Nu number compared to the base fluid, pressure drop or combination of these results
- Error estimation and repetition of tests

Generally, there are different mechanisms suggested for the anomalous enhancement of heat transfer like Brownian motion, interfacial layer theory, electrical double layer theory, aggregation and diffusion etc. which will subsequently be discussed.

1.1. Brownian motion

Brownian motion is a transport phenomenon in which small particles suspended in a stationary fluid move randomly, first observed by a Scottish botanist, Robert Brown in 1827 (Ford, 1992) and this theory was developed by Einstein's works, later on.

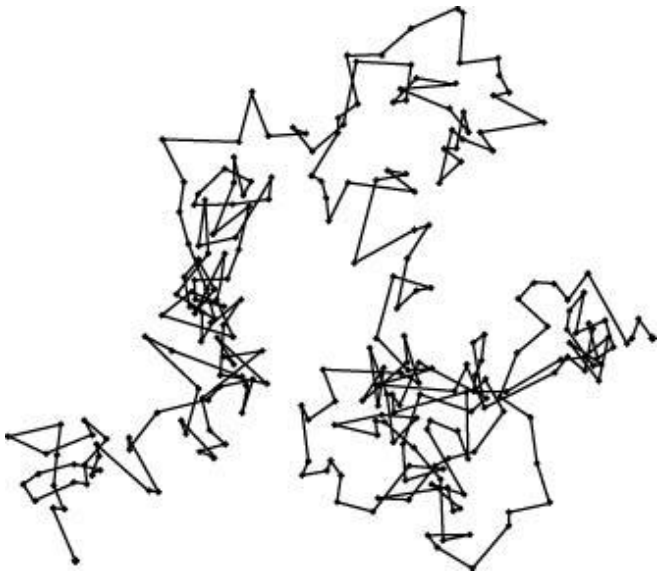

Figure 1. A schematic view of Brownian random movements of an assumed particle

Einstein's result (Einstein, 1905) for the diffusion coefficient D of a spherical particle which is a significant property of the motion of particles in the medium is defined as:

$$D = \frac{k_B T}{6\pi\mu r} \qquad (1)$$

where k_B represents the Boltzmann constant, T the temperature, μ the viscosity of the medium and r the radius of the particle. It can be understood from above equation, the smaller the size of the particle the more diffusion that particle has. Diffusion of particles also increases with decline of viscosity and increase in temperature. That is why Brownian motion is effective on small scale systems especially in higher temperatures with low viscid fluids and as a general rule, viscosity decreases when temperature increases which leads to increase in diffusion.

1.2. Interfacial layer theory (Kapitza resistance)

The Kapitza resistance is a thermal boundary resistance that is a measure of an interface's resistance to thermal flow and is generated when thermal energy carrier at an interface is scattered like what happens to phonons and electrons. The kind of carrier scattered is dependent to the materials controlling what happens in the interfaces. When there are nanoparticle-base fluid interfaces, for instance in liquid-solid interfaces the Kapitza resistance is assured to decline consequently the overall thermal resistance of the nanofluid (or generally the system) will reduce. (Meibodi et al., 2010)

1.3. Aggregation and diffusion

Aggregation and diffusion can be simply explained when nanoparticle chains formed together and make a linear assembly right after they are suspended in the base fluid. This chain assembly is assumed to escalate the heat propagation with faster thermal diffusion due to the providing a more rapid heat transfer path through the nanofluid. (Liao et al., 2003)

1.4. Electrical double layer (EDL) theory

The mechanism explained by EDL theory suggests a way to boost the heat transfer of molecules by a slight shift in the strength of intermolecular interaction forces that effectively alters the mean free path of the nanoparticles. (Jung and Yoo, 2009)

There were various types of nanoparticles used in previous works while magnesium oxide showed inadequate results, titanium dioxide caused some problems such as pipe clogging, silicon dioxide was chosen rather than alumina because of the promising results it had in one of the latest papers (Meriläinen et al., 2013)

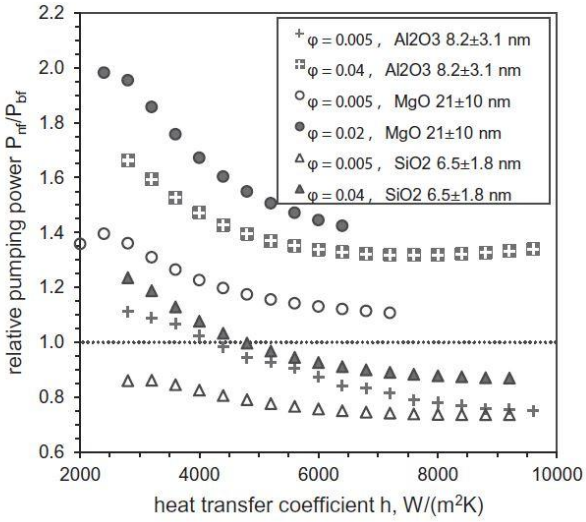

Figure 2. Relative pumping power P_{nf}/P_{bf} of several nanofluids as a function of the heat transfer coefficient (ibid)

Silicon dioxide is called by these names as well, Quartz, Crystalline silica, Cristobalite, Silicon (IV) Oxide, silane, Dioxosilane, Silica, dioxo and plainly Sand.

2. CONVECTION HEAT TRANSFER IN NANOFLUIDS

In this chapter, convection heat transfer in nanofluids is being discussed with the introduction of some frequently used parameters.

2.1. Dimensionless numbers

Definition of some dimensionless numbers

Buckingham π theorem is a great tool to use nondimensionalization for analysis of different phenomena in physics (White, 2003). In the following, some of the most important dimensionless numbers which have been used in this research will be introduced.

2.1.1. Reynolds number

Re is the ratio of inertial force to viscous force in a fluid. It is defined as:

$$Re = \frac{\rho VL}{\mu} = \frac{VL}{\upsilon} \tag{2}$$

where, ρ is the density of fluid, V is the velocity of flow, L is the characteristic length, μ is the dynamic viscosity and ν is the kinematic viscosity. The characteristic length is dependent upon the geometry of flow (Internal or external flow, geometry of pipe), for instance, for a closed tube or duct we have internal flow with the hydraulic diameter, D_h as the L. D_h is defined as the ratio of 4 times the area over the periphery which is the diameter of a circular pipe or the length of a square in a square duct as characteristic length.

$$\mathrm{D_h} = \frac{4\mathrm{A}}{\mathrm{P}} \tag{3}$$

For a circular pipe: $\mathrm{D_h} = \frac{4\mathrm{A}}{\mathrm{P}} = \frac{4\pi \mathrm{r}^2}{2\pi \mathrm{r}} = 2\mathrm{r} = \mathrm{d}$

For a square shaped cross section duct: $D_h = \frac{4A}{P} = \frac{4a^2}{4a} = a$

The lower Re shows more laminarity for the flow and the higher Re shows more turbulence for the flow which has different rules and correlations. Between these two regions, there is a transition region.

If we have developing flows or entry region the definitions of friction factor will be different.

2.1.2. Nusselt number

Nu is the ratio of convective heat transfer over conductive heat transfer. (Çengel, 2007)
So the bigger the Nu, the more convection there is compared to conduction. That means the fluid has more capacity to transfer heat through convection which is the dominant heat transfer mechanism in liquids and gases than the conduction which is more dominant in solid materials.

$$Nu = \frac{hD}{k} \tag{4}$$

Based on the Re that is the flow regime, there are correlations defined to find the Nu, like the ones below which are used in this research. (ibid)

Hausen

$$\overline{Nu}_D = \frac{3.66 + 0.0668\left(\frac{D}{L}\right)Re_D Pr}{1 + 0.04[\left(\frac{D}{L}\right)Re_D Pr]^{\frac{2}{3}}}, Re_D < 2300 \tag{5}$$

Sieder and Tate

$$\overline{Nu}_D = 1.86\left(\frac{Re_D \Pr}{\frac{L}{D}}\right)^{\frac{1}{3}}\left(\frac{\mu}{\mu_s}\right)^{0.14}, \begin{bmatrix} T_s = constant \\ 0.48 < Pr < 16700 \\ 0.0044 < \left(\frac{\mu}{\mu_s}\right) < 9.75 \\ Re_D < 2300 \end{bmatrix} \tag{6}$$

Gnielinski

$$Nu_D = \frac{\left(\frac{f}{8}\right)(Re_D - 1000)Pr}{1 + 12.7\left(\frac{f}{8}\right)^{\frac{1}{2}}(Pr^{\frac{2}{3}} - 1)}, \begin{bmatrix} 3000 < Re_D < 5 \times 10^6 \\ 0.7 \leq Pr \leq 16700 \end{bmatrix} \quad (7)$$

Dittus-Boelter

$$Nu_D = 0.023 Re_D^{\frac{4}{5}} Pr^n, \quad \begin{bmatrix} n = 0.4\ for\ heating \\ n = 0.3\ for\ cooling \\ 0.7 \leq Pr \leq 16700 \\ Re_D \geq 10000 \\ \frac{L}{D} \geq 10 \end{bmatrix} \quad (8)$$

If one can find the Nu, then using the equation 4, heat transfer coefficient can be derived.

2.1.3. Prandtl number

Prandtl number is another dimensionless number which is the ratio of viscous diffusion rate over thermal diffusion rate. (White, 2006)

$$Pr = \frac{\nu}{\alpha} = \frac{\mu c_p}{k} \quad (9)$$

where, ν is the kinematic viscosity, α is the thermal diffusivity, μ is the dynamic viscosity, c_p is the specific heat and k is the thermal conductivity. (Bohne et al., 1984)

Higher Prandtl number shows that momentum diffusivity dominates and lower Prandtl number shows that thermal diffusivity dominates. For instance, Mercury is a metal with high thermal conductivity which has dominant conductivity so Pr number is small for mercury.

For fluids with almost Pr=1 such as gases, thermal and velocity boundary layers coincide with each other.

2.2. Laminar flow

There are various definitions for flow regimes and range of Reynolds numbers.

For instance in an internal flow, Re<2100-2300 accounts for laminar flow. 2100-2300<Re<4000 depicts transition region and Re>4000 outlines turbulent regime. The differences between these regions are in friction factor and relative roughness of pipes in turbulent flows which will have effects on pressure drop.

We know that when the viscosity increases (as the only variable while the other parameters kept constant) pressure drop increases. The criteria of this research are the transition from laminar to turbulent forced flow in a horizontal circular tube when the flows are fully developed.

For internal Flow of a circular pipe (Çengel and Cimbala , 2010)

Re<2300	Laminar Flow
2300<Re<4000	Transitional Flow
Re>4000	Turbulent Flow

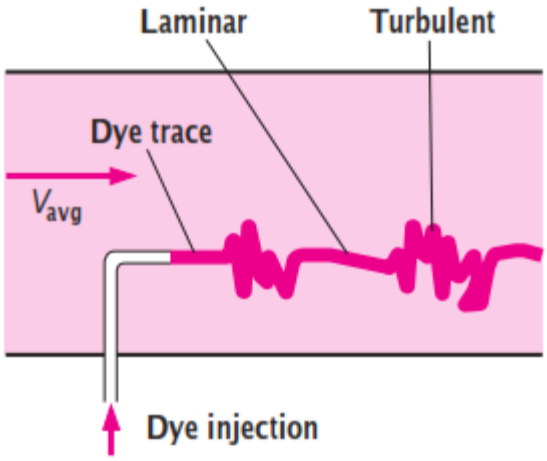

Figure 3. Trace of dye in laminar and turbulent flows

If the tube remains smooth and flow disturbance can be avoided, laminar flow can be achieved up to Re = 100,000 which is very hard to maintain in practice.

The characteristics of a laminar flow are as follows:

- Flow in layers parallel to boundary

- Low Re number
- From mixing point of view, it has small molecular diffusion
- Velocity profile is parabolic
- Shear stress is lower
- Solution to the flow is analytical

2.3. Turbulent flow

The characteristics of a turbulent flow are as follows:

- Higher Re number
- Resulted by the intricate interaction between the inertia terms and viscous terms existing in the momentum equations.
- Irregularity and randomness.
- Difficult full deterministic approach so these flows are explained using statistics
- Always chaotic (All chaotic flows are not necessarily turbulent since a turbulent flow is diffusive as well)
- Diffusivity causes fast mixing and increased rates of momentum, heat, and mass transfer
- Rotational with 3 dimensional vortices
- Dissipation of the flow which is conversion of kinetic energy to heat because of viscous shear stresses

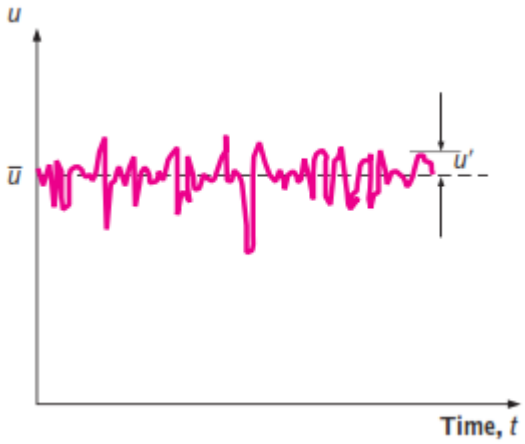

Figure 4. Fluctuation of velocities in a turbulent flow considering the mean velocity

The above figure shows the fluctuations in turbulent flow for the u as the velocity component with t as the time at a specified location.

2.4. Transitional flow

It appears that the transition from laminar to turbulent flows is also dependent on the fluctuations in the flow, pipe vibrations and roughness of the pipe as it can affect the degree of disturbance of the flow by surface roughness. In the transitional flow region, the flow switches between laminar and turbulent randomly. (ibid)

When one applies external disturbance, it can be observed that there are uneven fluctuations. Sporadic laminar and turbulent flow arise, i.e. phases take place that have characteristics of laminar flow and phases come up which have the attributes of turbulent flow.

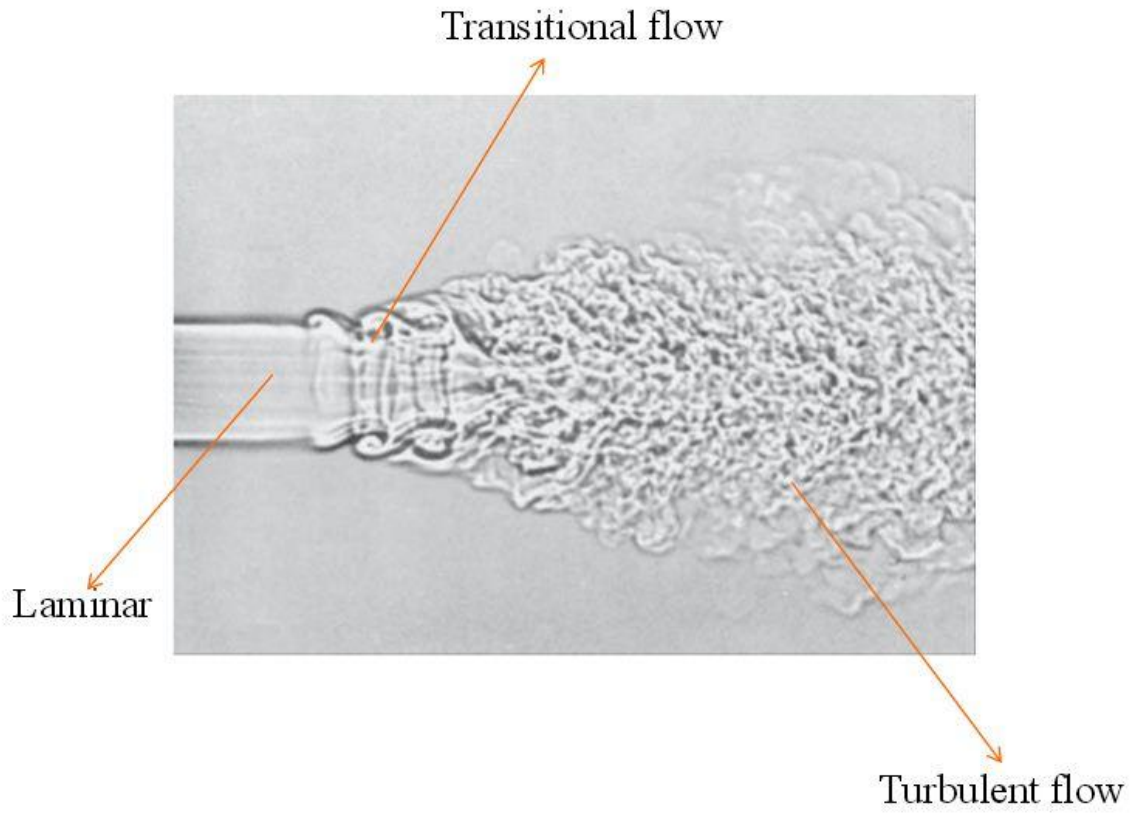

Figure 5. Areas of laminar, transitional and turbulent flow shown on a subsonic open jet

In a laminar flow, the velocity signal depicts a constant trend while in a turbulent flow, a time variation of the local velocity exists and one can observe the velocity fluctuations around the mean value.
We should note that the Re>2300 criterion is for circular pipes and is not the same for various pipe cross sections such as rectangular or flows surrounding a blade. Even for circular pipes 2300 is not necessarily absolute since this is dependant also on whether there is any disturbance present. This means that if the pipe is smooth and the experiment is done carefully we may reach higher degrees of Re in laminar region without the transition. On the other hand, if Re is less than 2300 no matter the disturbances exist the flow will be laminar.
In addition to what explained above, in transition region, for a fixed Reynolds number, friction factor increases with increasing Prandtl number. (Wang et al., 2013)

2.5. Governing Correlations

Generally we know that for fully developed turbulent flow with smooth pipe, the correlation for Nu is as follows (Çengel and Ghajar , 2011):

$$Nu = ARe^m Pr^n \tag{10}$$

(A is a constant, m and n are specified based on the heating and cooling conditions)

$$\dot{W}_{pump} = q\Delta P \tag{11}$$

Poiseuille's Law (Tuchinsky, 1976):

$$q = \dot{\mathrm{V}} = A.V = \frac{\pi D^4 \Delta P}{128 \mu L} \tag{12}$$

$$\dot{W}_{heat} = hA\Delta T \tag{13}$$

f is the friction factor and can be acquired from Moody diagram.

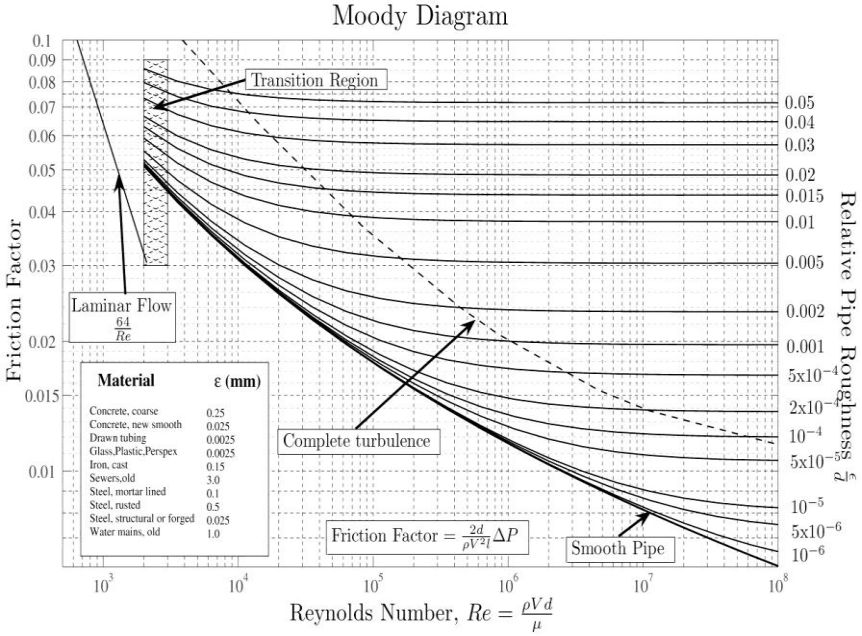

Figure 6. Moody chart showing friction factor plotted against Reynolds number for various roughnesses (Moody, 1944)

when μ increases and L, D and V_m are constant, pressure drop increases as in Darcy-Weisbach Equation:

$$\Delta P = f\frac{L}{D}\frac{\rho {V_m}^2}{2} = \frac{32\mu L {V_m}^2}{D^2} \quad (14)$$

We know in laminar flow based on Moody diagram:

$$f = \frac{64}{Re} \quad (15)$$

Whereas in turbulent flow:

$$\frac{1}{\sqrt{f}} = -2\log\left(\frac{\frac{\varepsilon}{D}}{3.7} + \frac{2.51}{Re\sqrt{f}}\right) \quad (16)$$

$$Nu = ARe^m Pr^n \quad (17)$$

For fully developed turbulent flow with smooth surface

$$Nu = 0.125RePr^{\frac{1}{3}} \quad (18)$$

$$Nu = 0.023Re^{0.8}Pr^{\frac{1}{3}} \quad (19)$$

when $0.7 \leq Pr \leq 160, Re > 10{,}000$

If T_s is constant:

$$Nu = 3.66 \quad (20)$$

If q_s is constant:

$$Nu = 4.36 \tag{21}$$

In turbulent flow f is dependent upon the smoothness or roughness of the pipe.

$$\dot{W}_{pump\ ,nf} = q\Delta P_{nf} \tag{22}$$

$$\dot{W}_{heat\ ,nf} = h_{nf} A\Delta T \tag{23}$$

We may define overall efficiency based on the overall effect of pumping power and heating power due to the use of nanofluids compared to the based fluid.

$$\eta = \frac{\dot{Q}_{NF}}{P_{Pump\ ,NF}} \times \frac{P_{Pump\ ,W\rightarrow NF}}{\dot{Q}_{W\rightarrow NF}} \times 100 \tag{24}$$

Table 1. Flow for circular tube

Range of Re	Nusselt Number
0.4-4	$Nu=0.989\ Re^{0.330}Pr^{1/3}$
4-40	$Nu=0.911\ Re^{0.385}Pr^{1/3}$
40-4000	$Nu=0.683\ Re^{0.466}Pr^{1/3}$
4000-40,000	$Nu=0.193\ Re^{0.618}Pr^{1/3}$
40,000-400,000	$Nu=0.027\ Re^{0.805}Pr^{1/3}$

2.6. Annulus Heat Transfer

In the next step, some kinds of correlations were derived from literature to calculate the heat transferred in the annulus between two tubes. For the default mode of the setup, water flows downward and nanofluid flows in the upward direction, so the flow of heat exchanger is counter flow.

In this section, some of the governing equations for two concentric tubes that used in this research are introduced.

For concentric cylinders which set horizontal with the diameters of D_o, D_i, natural convection heat transfer rate through the annular space is as follows: (Çengel, 2003)

$$\dot{Q} = \frac{2\pi k_{eff}}{\ln(D_o - D_i)}(T_o - T_i) \qquad \left(\frac{W}{m}\right) \tag{25}$$

where effective thermal conductivity is: (Raithby and Hollands, 1975)

$$\frac{k_{eff}}{k} = 0.386\left(\frac{Pr}{0.861 + Pr}\right)^{0.25}\left(F_{cyl}\,Ra_L\right)^{0.25} \tag{26}$$

where the geometric factor F_{cyl} is:

$$F_{cyl} = \frac{[ln(D_o - D_i)]^4}{L_c^3\left({D_i}^{-0.6} - {D_o}^{-0.6}\right)^5} \tag{27}$$

where L_c is the characteristic length:

$$L_c = \frac{(D_o - D_i)}{2} \tag{28}$$

which is valid for 0.7<Pr<6000, $100 < F_{cyl}\,Ra_L < 10^7$

Most articles observed, did not take the convective heat transfer parameter into account.

Natural convection heat transfer for the nanofluids in annular spaces which are flowing between the two horizontal concentric cylinders (Cianfrini, et al., 2011)

$$q = 0.386\frac{2\pi Lk(T_i - T_o)}{b^{3/4}(1/{D_i}^{3/5} + 1/{D_o}^{3/5})^{5/4}}[\frac{PrRa_b}{0.861 + Pr}]^{1/4} \ ,$$
$$0.7 \le Pr \le 6000, \frac{[ln(D_o/D_i)]^4}{b^3(1/{D_i}^{3/5} + 1/{D_o}^{3/5})^5} Ra_b \le 10^7 \quad (29)$$

which is the same as the first correlations. In this article, they combined all in one. This was used to see the effect of forced convection to compare with natural convection.

$$\Phi_{tot} = \dot{m}cp\Delta T \quad (30)$$

$$\Phi_{tot} = \Phi_{amb} + \Phi_{NF} \quad (31)$$

$$\Phi_{NF} = \dot{m}_{NF}cp\Delta T \quad (32)$$

$$\Phi_{amb} = \frac{kA\Delta T}{\Delta x} \quad (33)$$

Natural convection heat transfer coefficient from insulation to the ambient

$$h_{ambient} = 5\frac{W}{m^2K} \quad (34)$$

Insulator is made of polystyrene

$$K_{insulator} = (0.035 - 0.040)\frac{W}{mK} \quad (35)$$

3. CHARACTERIZATION OF NANOFLUIDS

For the sake of making sure that nanoparticles' sizes and distributions are as claimed by the manufacturers and to find some of the necessary properties of nanofluids, the following steps should be taken.

3.1. Usage of Dynamic Light Scattering (DLS) device

DLS (dynamic light scattering) device was used in order to measure the size of the nanoparticles dispersed in base fluid to check out whether the announced size is the same as the real size or not. Actually, this is critical to make sure since some manufacturers claim some sizes that are not right and can conclude to wrong results if not tested beforehand.

This step can be taken into account as the preparation stage which can be developed by mixing the nanofluid using ultra sound device that can be used with the magnetic stirrer if there is a limitation of lowering the ultra sound tip deep into the fluid. Actually, sonication has different options based on the application expected. User can change the magnitude and cycle options that are scaled respectively from 0-100 and 0-1.

In order to use the DLS device to obtain more precise results, one can employ other methods such as pH adjustment and addition of surfactants. However, surfactants are added when phase change such as melting occurs which is not applicable in the current research.

There are different acronyms representing by various authors pertaining to the same definition. PCS (Photon Correlation Spectroscopy), QELS (Quasi-Elastic Light Scattering) and IFS (Intensity Fluctuation Spectroscopy) are other terms for DLS. (Tscharnuter, 2006) Basically, this method measures Brownian motion and relates this to the size of the particles with a laser and analyzing the intensity fluctuations in the scattered light.

DLS measurements are done using the instrument from Malvern Instruments Limited Company.

3.1.1. PdI (Polydispersity Index)

PdI is a dimensionless index which is a calculated number based on a fit to the correlation of data of cumulant analysis (based on a simple method of autocorrelation function which is generated by a DLS experiment). PdI is scaled in a way that "values smaller than 0.05 are rarely seen other than with highly monodisperse standards." (Xu, 2001) (Murashov and Howard, 2011)
If the values are greater than 0.7 they would show that "the sample has a very broad size distribution and is probably not suitable for the DLS technique. The various size distribution algorithms work with data that falls between these two extremes." (Dahneke, 1983) (Pecora, 1985)

There are three different cases in PdI which has been interpreted as follows
Case (a) with one peak, in this case, PdI is close to 0
Case (b) with two or more peaks, in this case PdI is close to 1 which is not desirable.
Case (c) with two peaks which has a deep valley which is better than case b, however, it is not acceptable enough.

3.1.2. Z-Average

DLS results are described with Z-Average which is not affected by the noise since it is a mathematically stable parameter. Therefore, this parameter is more preferable than ordinary size. Then, Z-Average is the intensity based harmonic mean. (Washington, 1992)

$$D_z = \frac{\Sigma S_i}{\Sigma (S_i / D_i)} \qquad (36)$$

where S_i represents the scattered intensity from particle i and D_i stands for the diameter of particle i. (Hackley and Clogston, 2010)

since we have very small particles, Rayleigh scatterers can be applied (Thomas, 1987). $S_i \sim D_i^6$

$$D_z \approx \frac{\Sigma D_i^6}{\Sigma D_i^5} \quad (37)$$

“Despite the convoluted meaning, the Z-average size raise with the increase in particle size. Thus, it gives a reliable measure of the average size of a particle size distribution in addition to being easily measured. Because of those reasons, the Z-average size has become the accepted norm for presenting particle sizing results by DLS”. (Pecora, 1985)

There are various terms such as number distribution, intensity distribution and volume distribution which can be depicted as the results of Z-average. Intensity distribution has the highest peak among those. The second highest peak belongs to the number distribution, while the lowest peak corresponds to volume distribution.

a) Intensity Distribution

Intensity distribution of particle sizes is the first order outcome from a DLS experiment. It is weighted based on the scattering intensity of each particle fraction or family. The particle scattering intensity is proportional to the second power of the molecular weight for biological materials or polymers.
So the results from an intensity distribution can be trumped-up if a small amount of agglomeration/aggregation or existence of a larger particle species may dominate the distribution. However, this distribution turns out to be an indicator or as a sensitive detector for the existence of a large material in the sample.

b) Volume distribution

The main size distribution produced by a DLS device is intensity distribution; however, it can be converted to volume distribution using Mie theory. Volume distribution is based on the relative proportion of different components of a sample based on volume or mass instead of intensity (their scattering) 4 assumptions should be considered while this transformation is carried out:

1. No error exists in the intensity distribution
2. All particles are homogeneous
3. All particles are spherical

4. The optical attributes of the particles are known, that is the imaginary and real components pertaining to the refractive index.

3.1.3. Zeta potential

When a particle is dispersed in a liquid or emulsion and it has an electric charge, it will be surrounded by a thin layer which is mostly comprised of the opposite charge, since opposite charges always attract each other. After this layer, a wider layer is formed which is more diffused than the first layer. The bulk of the liquid has its own electrical charge, as well. Zeta potential is the voltage difference between the thin layer and the fluid bulk. It is always negative in aqueous colloids and is usually measured in millivolts between -14 to -30 mV. When the electronegativity is high enough there can be always a negative repulsion that makes the particles to repel each other not to sediment or agglomerate. This means that for those Zeta potentials, the dispersion is stable. The range of stability can be assured within -45 to -70 mV. When aggregation is appealing, zeta potential values are appropriate when are closer to zero.

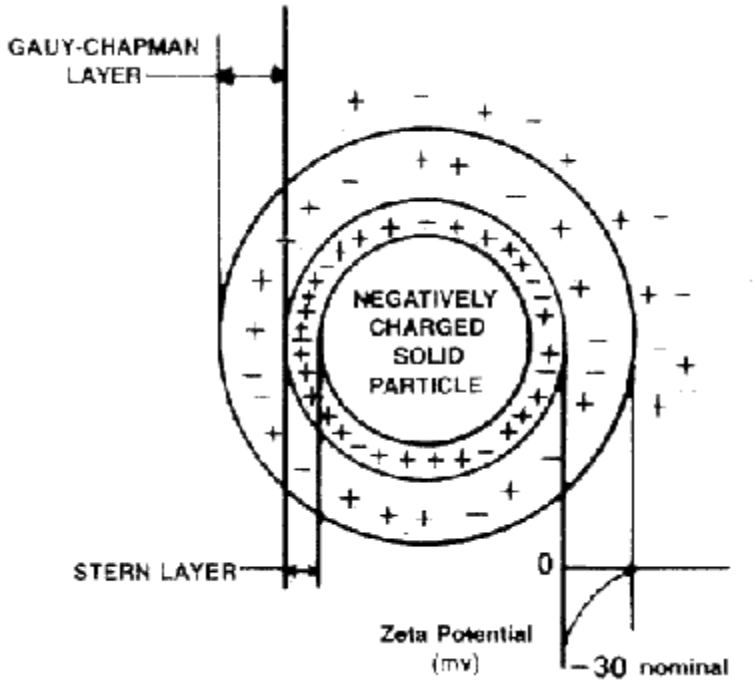

Figure 7. Schematic figure of zeta potential surrounding a colloid

3.2. Differential Scanning Calorimetry (DSC)

Specific heat was measured using DSC device. Differential scanning calorimetry is a method to obtain specific heat capacity of a sample by employing a thermoanalytical technique. The measurement device is manufactured by NETZSCH.

In order to measure the specific heat capacity with differential scanning calorimetry, the sample should be put on a very tiny pan and compress the lid over the pan to prepare it for the experiment. At first to calibrate the device in terms of accuracy and repeatability, the specific heat is measured for known materials such as sapphire disk. (Thomas, 2003)

DSC measures the amount of energy absorbed or released by a sample when it is heated or cooled, as if it is producing extra heat or absorbing extra heat, providing quantitative and qualitative data on exothermic or heat evolution and endothermic or heat absorption processes.

3.3. Falling ball viscometer

Viscosity Measurements are done using the falling ball viscometer manufactured by Thermo Electron Corporation called HAAKE Falling Ball Viscometer Type C. The ball chosen for measurements is Ball no.1 since water based nanofluids have the viscosities a bit bigger than water which falls in the range of 0.6-10 mPa.s.

It measures the viscosity by measuring the time needed for a ball to fall from a specific line to another one in a tube which has slightly bigger diameter than the ball. The tube is located with a slope of 10° compared the perpendicular axis to the table.

$$\mathrm{K}_{return} = \frac{\text{normal falling time} \cdot \text{ normal constant K}}{\text{falling time when returning}} \tag{38}$$

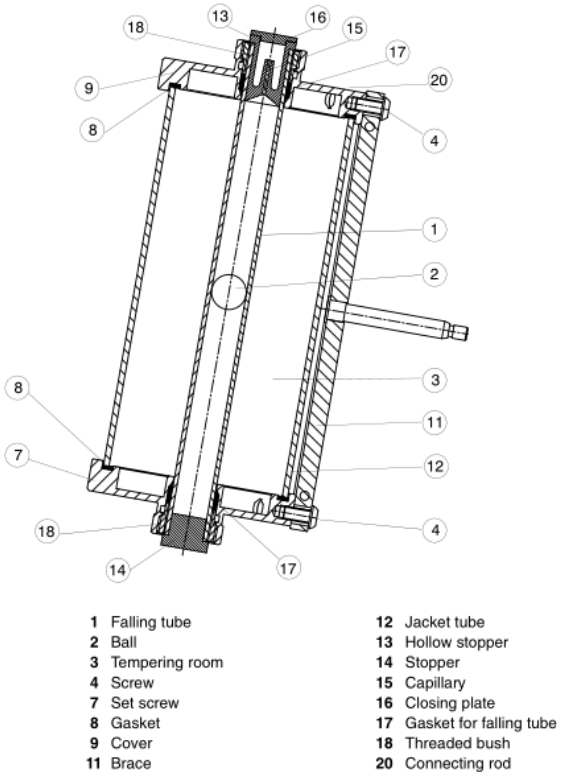

Figure 8. Components of the falling ball viscometer

3.4. Thermal conductivity measurement

Thermal conductivity has been measured by the instrument located in the chemistry department of Aalto University using Hot Disk technique. It works only in the room temperature; therefore, to obtain the thermal conductivity in various temperatures, it was supposed to follow the pure water trend.

4. EXPERIMENTAL SETUP

In this chapter, the components of experimental setup will be introduced along with its geometries and challenges one should deal with in practice including replacing the fluid, degassing the pipes and safety instructions.

4.1. Setup components

At first, based on the present experimental setup which consists of the following items:

- An insulated tank which is full of water to heat up or cool down the nanofluid sample.
- Electrical heater which heats up the tank
- Two sets of pumps (one for the tank flow and the other for the nanofluid flow) for nanofluid, there can be used two pumps one for slower flow and one for faster flow which were called laminar (less powerful) and turbulent (more powerful) pumps, although, with the laminar pump one can reach the turbulent region and with turbulent pump laminar region is accessible.
- Eight thermometers, T1 before heat exchanger, T2 right before heat exchanger, T3 right after heat exchanger and T4 after heat exchanger. T8 measures the tank temperature (on top of the tank, on left hand side). T9 is the tank water temperature right after test section which is located right before entrance of the tank and T10 is the tank water temperature right before test section which is located between tank and upper part of test section, after the tank. T5 measures the temperature in viscometer. (T9 should be higher than T10 in heating state and lower than T10 in cooling state)
- Right valve which guides the tap water to tank (RV), middle valve which guides the tap water to the Haake pump (MV) and left valve which provides water flow for viscometer (LV)
- One thermostat to keep the tank temperature on a specific value for stabilization of the flow (it was converted to an aggregated heater and thermostat during the progress of experiments)
- One pressure meter sensor which measures the pressure difference before and after heat exchanger

- The heat exchanger which consists of two concentric vertical pipes in which the inner pipe is made of copper and nanofluid is flowing in, while, the outer tube is made up of stainless steel and water is flowing in. Those pipes are covered very well with insulation material which is black polystyrene
- Three critical points (which are T shaped) and are used to degas the system when some bubbles form naturally. These stations capture and store bubbles to degas the system later on.
- One valve to insert pressurized gas to the system which was compressed air at first, then a compressed vessel of CO_2 was added to the equipment, which was used after all.
- Some pipes for connecting and creating a closed cycle.

A schematic view of the whole setup is presented in the following figure:

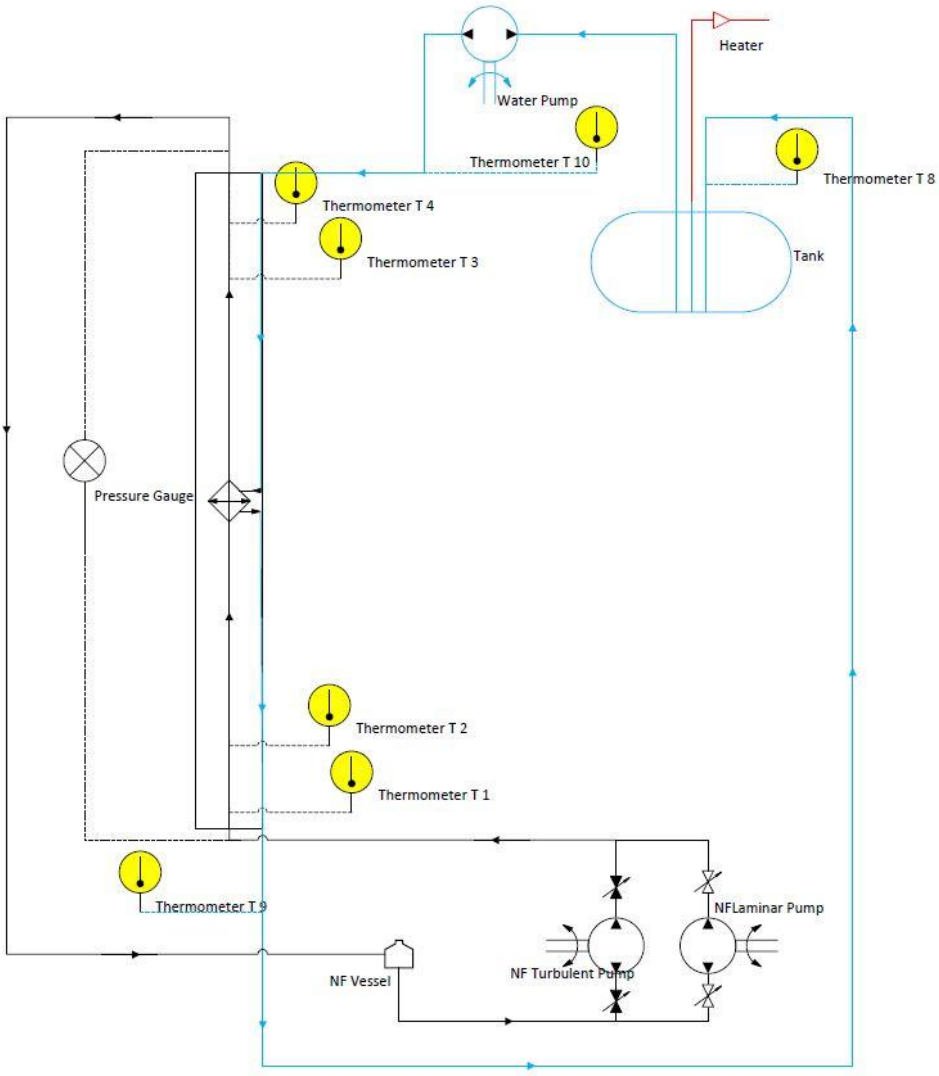

Figure 9. A schematic view of the experimental setup used to heat up the nanofluid

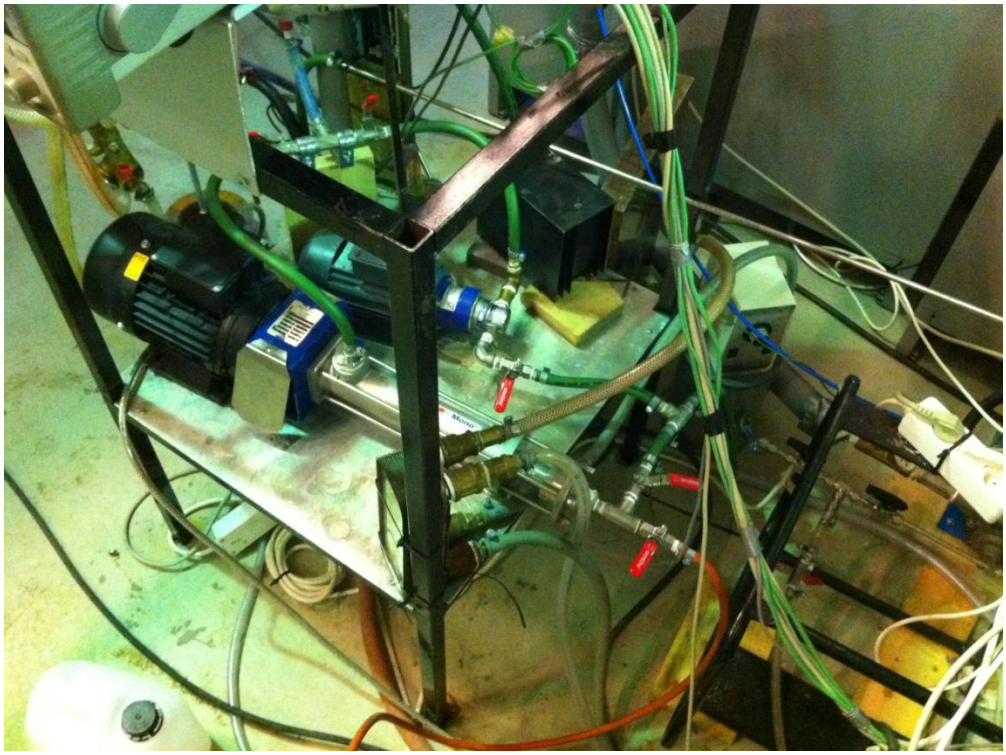

Figure 10. Experimental Setup (Pumps and Valves)

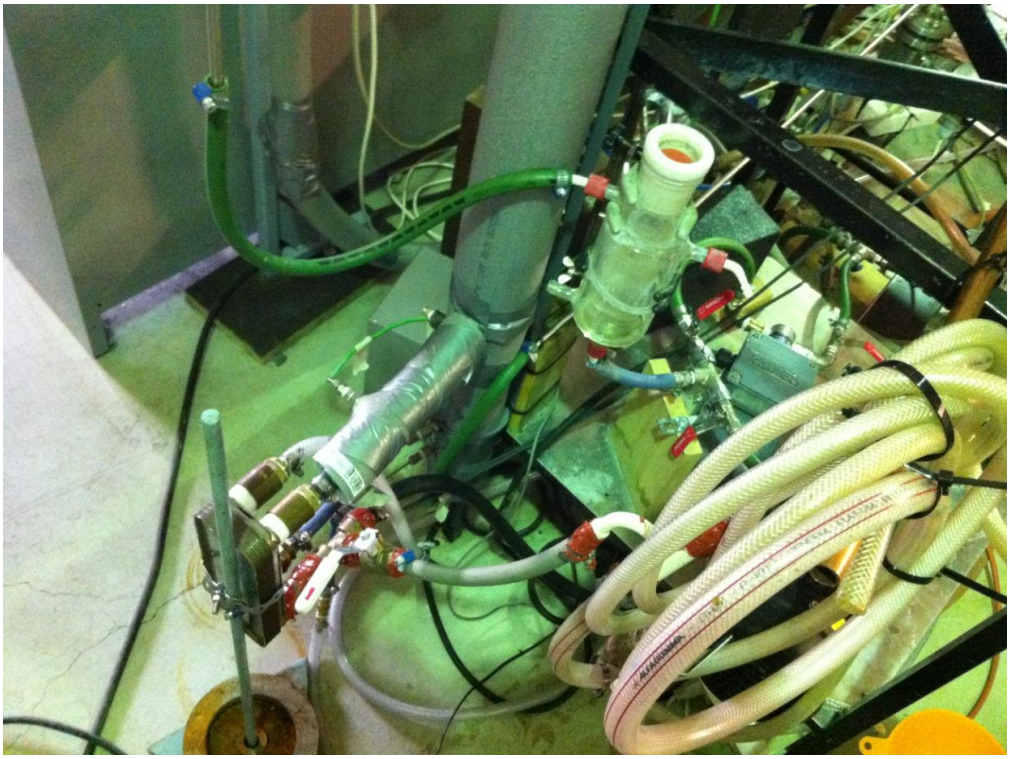

Figure 11. Experimental Setup (Heat Exchanger and nanofluids reservoir)

Figure 12. Experimental Setup (Vertical Heat Exchanger)

4.2. Geometries of setup

Some geometries of the setup which are important for measurements are as follows:

Table 2. Geometries of the experimental setup components

Abbreviation	Description	Size
L	length of the heat exchanger	1.47 m
L_p	length in which the pressure drop measurement occurs	1.68 m
d_i_o	inner diameter of the outer tube	8 mm
d_i_i	inner diameter of the inner tube	6mm
d_o_i	outer diameter of the inner tube	8mm
d_o_o	outer diameter of the outer tube	13mm
d_h	hydraulic diameter	13-8=5 mm

4.3. Challenges

4.3.1. Bubbles and degassing the system

There was some instability due to the formation of bubbles. These bubbles increase pressure drop and decrease the flow rate. This mostly happens when flow is so laminar that the stabilization time increases which consequently results to gradual decrease of flow rate until the measured value by the flow meter shows 0 or fluctuating around zero which can be explained by the natural convection due to the temperature difference and pump just works without effective pumping.

There are some useful points in degassing the system like:

1. It’s better to use both pumps for degassing the system since they have more power together.
2. Start the pump(s) with the highest speed.
3. Degassing should be repeated over and over again until you make sure that there is no bubble coming out of the small hose located in the T-shape on top of the apparatus.
4. There are two other points for degassing the system, such as at the drainage tube that should be degassed.
5. Flow meter should be degassed with opening its two screws and closing them.

(It should be mentioned that flow meter has been put inside a metallic cage to remove the induction of electromagnetic effects which can alter the measured data and cause error).

4.3.2. Drainage of nanofluid

There are some useful points in draining the nanofluids:

1. Run the pump(s) with the highest speed.
2. The operator should hold a bottle or beaker below the tube to collect the nanofluid (not to waste it) since it is needed for further experiments to validate the results.
3. Wait and collect as much nanofluid until you feel that the pump is about to suck the air.
4. Then, shut off the pump quickly to avoid pump malfunction.
5. After most of the nanofluid has been drained out of the pipes, some small amount that requires compressed air or pressurized CO_2.
6. Open a little bit the pressurized CO_2 valve and watch nanofluid exiting. One must make sure not to increase the pressure which can disturb the fittings and joints.
7. There should be no fluid after all in the pipes.

4.3.3. Refilling the pipes of nanofluid

After washing the system quite well, suppose that the setup is at the state 1 of the previous procedure. Next, one can fill in the reservoir with as much nanofluid as it allows accepting without leakage. Set the pump on a very low frequency (20-30 Hz) and turn it on. Pump frequency can gradually increase to 100. Watch the reservoir carefully to add the nanofluid as soon as you see that nanofluid level surface is going down until you make sure there is no more nanofluid required.

If only turbulent pump is used, about 600 cc is enough to fill the system in. (before using the heat exchanger it needed 600cc, but after that, 200 cc more fluid needed because of the heat exchanger)

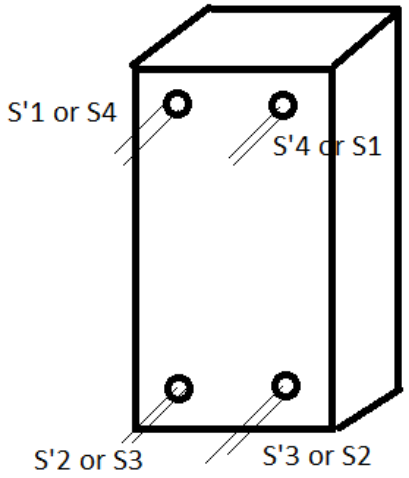

Figure 13. New heat exchanger

It is important to know that each sample's size and distribution should be checked before and after heat exchange test in order to approve the stability of nanofluid after heat exchange process.

Step by step guide to do the two aforementioned tasks which are degassing the pipes and drainage of nanofluid are available in the appendix.

4.3.4. Washing the system

In order to wash the tubes, one should wash the system with distilled water for several times to assure there is no significant amount of nanoparticles inside. To wash the interior part one would need distilled water and fill in the reservoir. Next, the pump should be turned on and water should be added gradually until make sure that the system is full of liquid. In this stage, it does not matter how many air bubbles there are in the pipes. So, the system can run for a few minutes and therefore the procedure (in the appendix) can be applied for several times to assure that even if some nanoparticles still remained they are diluted enough to be negligible. After a few times some dilute acids or bases can be used to help wash it better (depending on the samples can vary).

4.3.5. Comparison of pressurized CO_2 and air for evacuation of nanofluid

More bubbles were drained out of the system and caused better stabilization when CO_2 was used. This effective performance may be explained by the less molar mass of air compared to carbon dioxide, 29

to 44 g/mol respectively. At some points, it seemed that nanofluid flow meter shows more stabilized values when using pressurized CO_2 compared to compressed air.

4.3.6. Stabilization and temperature control

When a variation is exerted into the constant variables of a system, for instance, turbulent pump frequency or tank temperature alters, system needs time to accept the change to become time independent (steady state) that is stabilization. The smaller the flow rate the longer it requires waiting while the bigger flow rate entails shorter time in order to achieve stabilization. Temperature of the tank flow is being consistently controlled using a thermostat (for most cases on 80 ^{o}C). The set temperature can vary more when tap water bath is used to bring about bigger range of temperature difference for the inlet and outlet NF side.

4.3.7. Safety precautions

Nanoparticles can be dangerous when the material is poisonous to the human body, even if the material is not hazardous for health, due to the small size they can enter the cells when inhaled or if touched the wounds.

Of course, different nanomaterials have different impacts on health. Usually, the skin is a good protector against these materials. For this research, silica's characteristics have been investigated. "The results confirm that NPs are too large to permeate skin by this mechanism" (Watkinson et al., 2013), so there seems to be no danger working with them if the nanoparticles are not inhaled. For that purpose, the operator should work under a fume hood wearing gloves and a mask.

5. PREPARATION OF SAMPLES

In this chapter, the essential stages are introduced in order to prepare former silica/water nanofluid samples.

5.1. Weighing

In order to obtain the exact concentration of samples especially when dilution or enrichment is going to be carried out, one needs to weigh the containers without and with samples to make the further calculations. There are two or three different scales available in the lab with various maximum limits (for instance 200 g for one scale)

5.2. pH adjustment

Sometimes sedimentations can be avoided by adding acidic or basic compounds to nanofluid. It was done on three similar samples of silica, one acidic (pH~3), one basic (pH~10) and one neutral. Then results were compared which did not lead to any improvement.

5.3. Sonication of dispersion

Sonication is the process of applying sound energy to shake and mix the particles in a sample quickly, for different purposes. Frequencies used usually are ultrasonic, hence that is why this act is also known as ultra-sonication or ultrasonication (Lin et al., 2009). Different samples were tested using sonication device to mix the suspension more and help the colloids to disperse homogenously. In order to do that, one should prepare the fluid and test a sample beforehand by DLS device to compare afterwards. Then, the tip of sonicator shall be positioned a few centimeters over the bottom of the container to carry out the stirring more effectively. Then, the tip of sonicator will start rotating based on the application with various speeds or frequency. We should note that the stirring will produce heat that can cause the

beakers to break. So we should make sure the beakers are heat resistant.

5.4. Dilution of SiO2 dispersion sample

Since it was hard handling and working with the solid nanoparticles especially when sonication and pH adjustment did not solve any problems of sedimentation and agglomeration, it was decided to dilute the high concentrated dispersion sample which was 20% vol of silica into the water. As far as the surface of dispersion which was not used for a year or so was covered with some dust or dirt, it needed to be filtered to make sure that the sample is exactly at the promised size and distribution. Those dirt and grime were supposed to be bacteria or algae growing there. The calculations and weight measurements which was done precisely lead to 3 different samples will be explained in the next chapters.

5.5. Cooling down the nanofluid before test section with tap water bath

For cooling down the tank water, one should open the tap water, open one of the valves (there are three valves, one is to cool down the tank temperature which should be closed, the other is for viscosity cycle and the third one is the water valve for cooling cycle, called water bath) which cools down the nanofluid before entering the test section as much as it provides the highest possible temperature difference between inlet and outlet as long as the system is stable. Cooling section consists of a plate heat exchanger between inlet of nanofluid and tap water to cool it down before the main heat transfer section.

This makes higher temperature difference between inlet and outlet temperatures of nanofluid side. The more the temperature difference is, the more viscosity variation occurs within the nanofluid heat exchange section. This can cause the change of flow regime from laminar to transition or even turbulent if the temperature difference is high enough. As it was mentioned in previous sections, the main purpose of this study was to scrutinize the transition phase especially when a regime change occurs due to the significant temperature difference within the test tube than can alter the viscosity substantially.

6. MEASUREMENT OF NANOFLUIDS PROPERTIES

In this chapter, all the measurements have been introduced using their relevant measuring instruments including their calibration.

6.1. Calibration of flow meter for tank flow

Tank flow meter shows quite a stable value on the device, however, the settings value shown on computer outlines the output values are in ampere not volumetric flow (with a minus value). This means that this flow meter could have been calibrated if the sensor was assigned appropriately to the flow meter, however, since the values of flow meter are for instance in the range of 5.72-5.76 L/min, which is 0.3% variation from the average which is negligible and does not seem to be necessary to carry out.

6.2. Calibration of pressure meter

In order to get more reliable results with pressure meter, we should calibrate it using the column of water technique.
The difference in fluid height in a liquid column is proportional to the pressure difference.

$$h = \frac{P_a - P_o}{\rho g} \tag{39}$$

Where P_a is the measured pressure in the variable liquid heights and P_o is the measured pressure in the zero height.

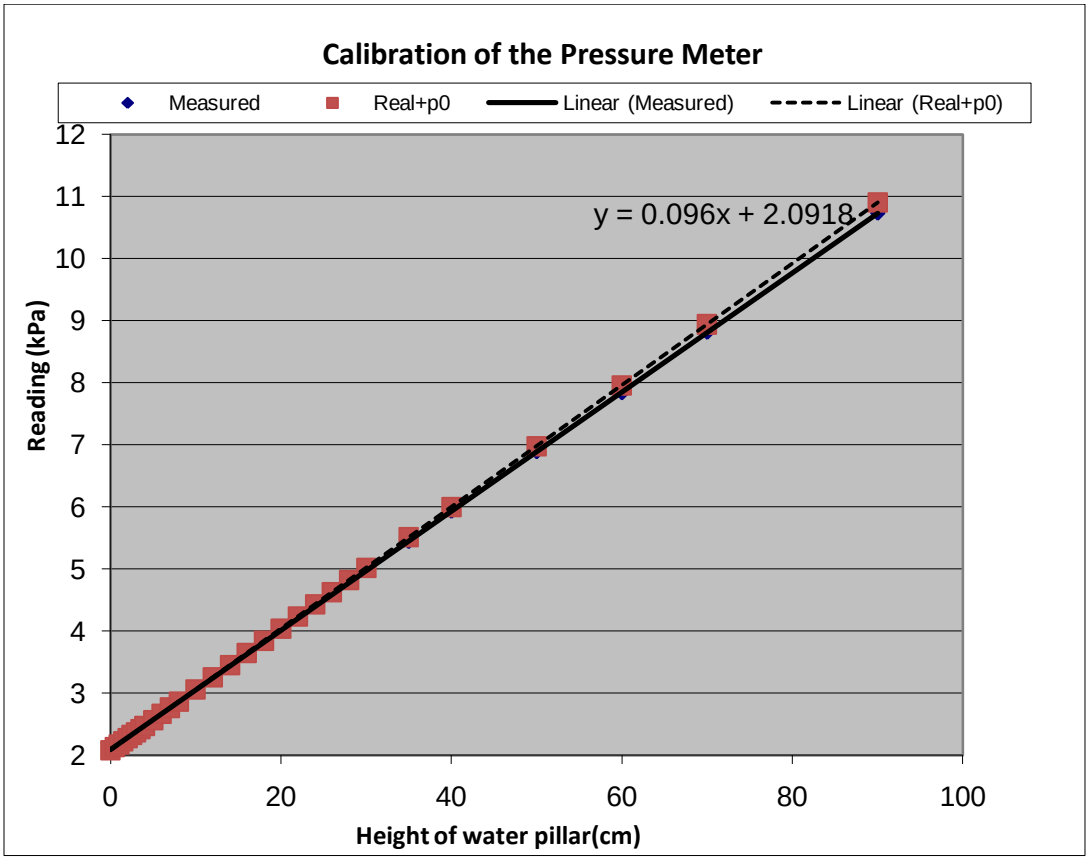

Figure 14. Calibration of the pressure meter

6.3. Heat transfer measurements

It's good to use 0.1% weight of Al_2O_3 and SiO_2 with water. Based on the literature, silica has better performance compared to alumina and especially compared to MgO, especially with much diluted samples. (Meriläinen et al., 2013)

The inner tube is made of stainless steel and the outer tube is made up of copper

- 13mm inner diameter of the outer tube
- 8mm outer diameter of the inner tube
- 6 mm inner diameter of the inner tube

$$d_h = d_a - d_i = 13 - 8 = 5\ mm \quad (40)$$

At first, it was guessed the water properties are still in the same one 1 bar pressure which are not,

however, they do not vary more than 1 percent, so they seem accurate enough. However, the correlation of water properties using 10 or more valid data was found and used as the water properties.

For silica sample the best results of heat transfer coefficient are with the smallest and the roundest particles. (ibid)

HTC in the Reynolds range of 500-4000 (the Reynolds number is minimum where it has lower temperature whether it is cooled in the inlet or it has been cooled naturally through the pipes)

1) Heating up (Tank temperature set on 95 ^{o}C)
   However, due to the slow convergence, it took so long to stabilize and reach that temperature so thermostat was set on 90 ^{O}C and practically tank temperature was about 88 ^{o}C.

2) Cooling down (with 15-20 Celsius tap water) using plate heat exchanger

Table 3. Three desired nanofluid volume percent concentrations

Sample Number	Volume concentration
1	0.1%
2	0.5%
3	2%

Since 2% vol sample had high pressure loss the higher concentrated sample was not produced. So, initially experiments with water as the base fluid should have been done and the best results will be repeated with ethylene glycol and water solution (before the change of plan)
Then it was decided to consider the transition region for 8 different points in the range of 2000-3000 with some points outside this interval and using silica in water instead of EG.

6.3.1. Water reference measurements

Next, some experiments were undergone using water reference measurements as nanofluid to check the

accuracy of measurements of the experimental setup. These measurements were done using either of the laminar and turbulent pumps.

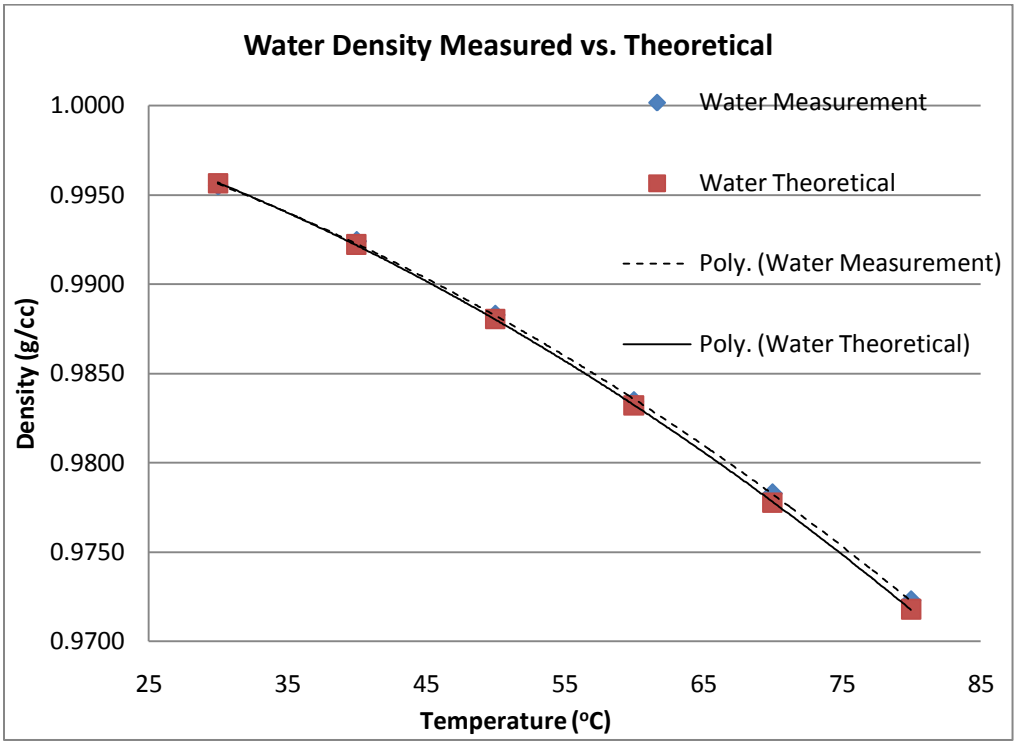

Figure 15. Density of water vs. temperature

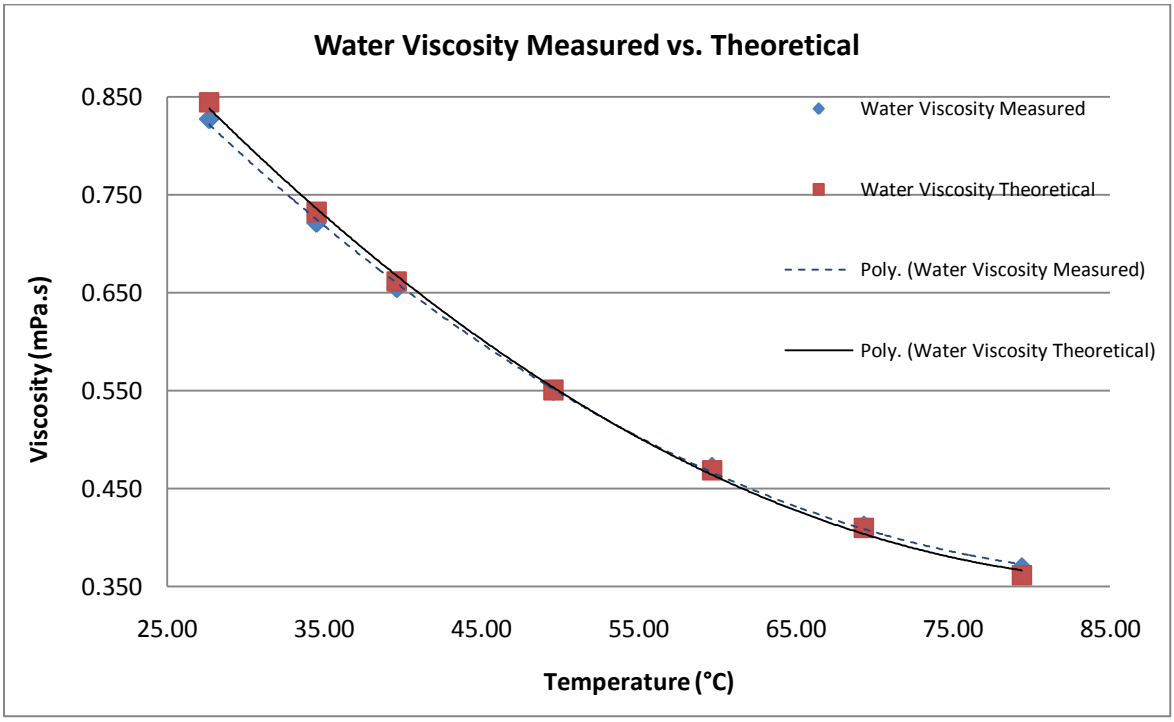

Figure 16. Viscosity of water vs. Temperature

6.3.2. Aluminum Oxide sample

DLS measurements were done at first on some alumina samples in the meantime of silica samples arrival. Based on the DLS results, alumina samples had higher PdI, which were not suitable to make the experiments.

6.3.3. SiO2 solid nanoparticles

In here, density, viscosity, thermal conductivity and specific heat of all silica samples are presented with a comparison to the water measurements:

6.3.3.1. Density measurements of SiO_2 samples

Densities have been measured by the hydrometer which works according to the buoyancy effect. The denser the fluid it is the floating glass will sink less and density can be read like the below picture.

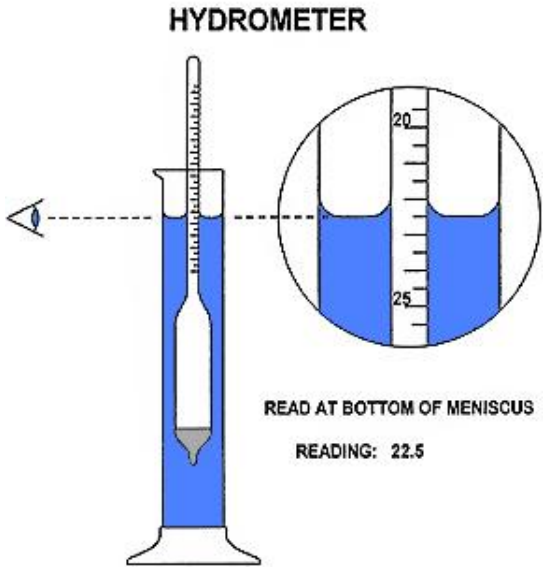

Figure 17. Sample picture of a hydrometer

Now the measured densities will be presented one by one:

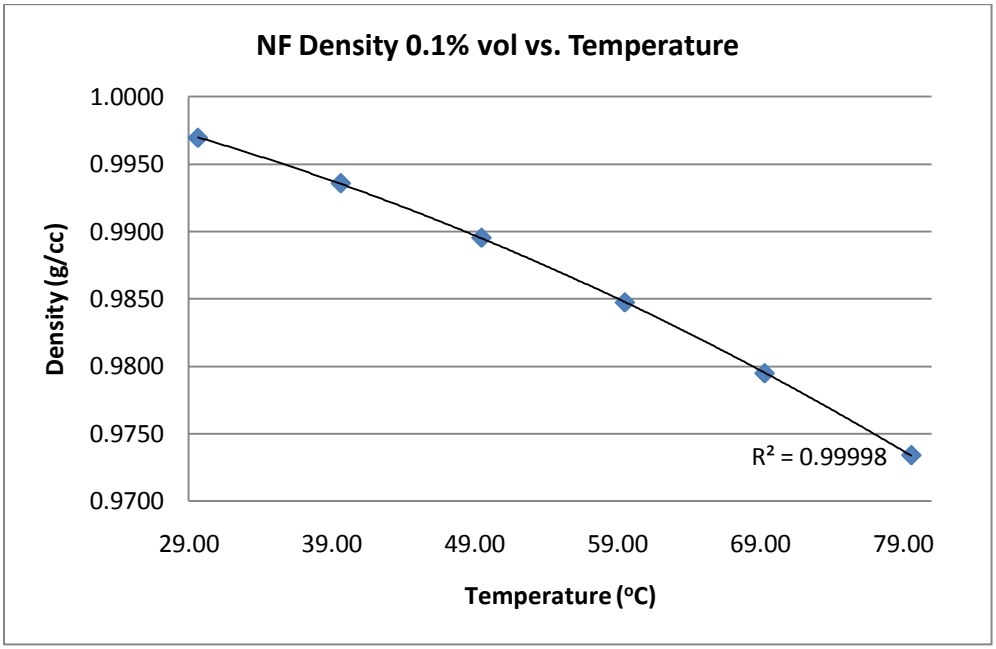

Figure 18. Nanofluid Density of 0.1% vol sample vs. Temperature

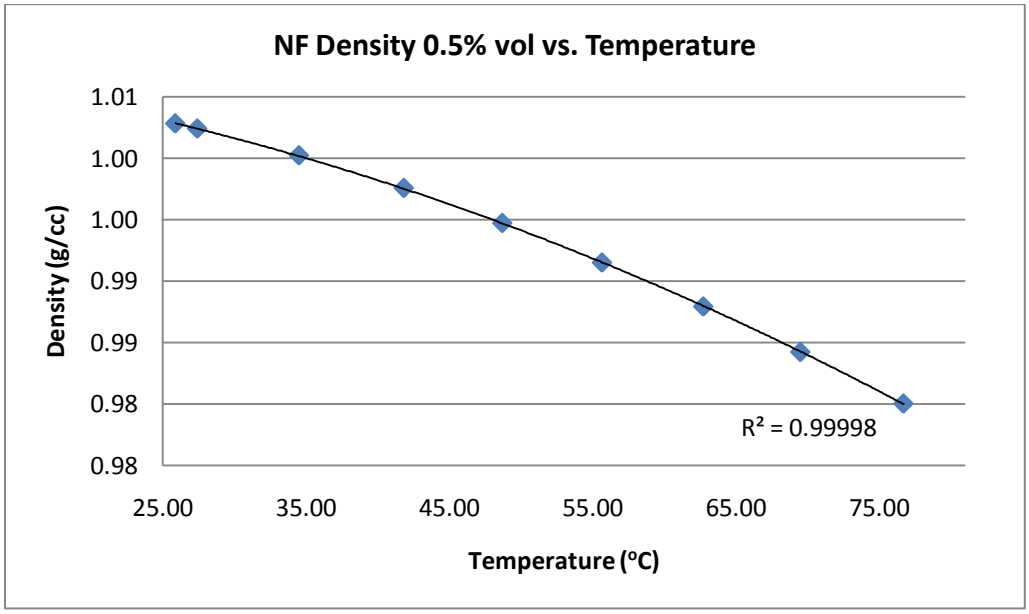

Figure 19. Nanofluid Density of 0.5% vol sample vs. Temperature

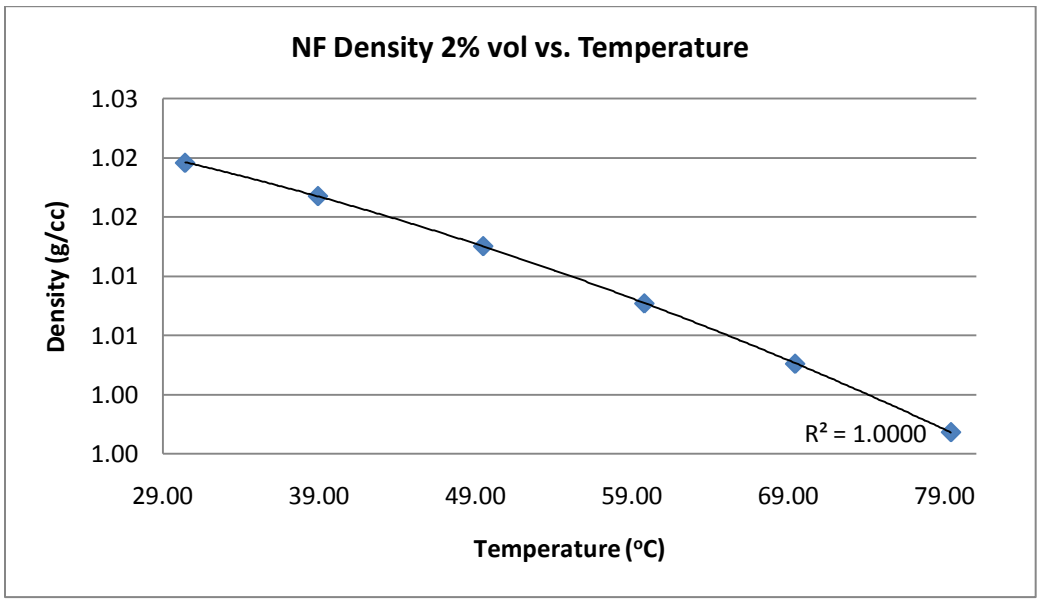

Figure 20. Nanofluid Density of 2% vol sample vs. Temperature

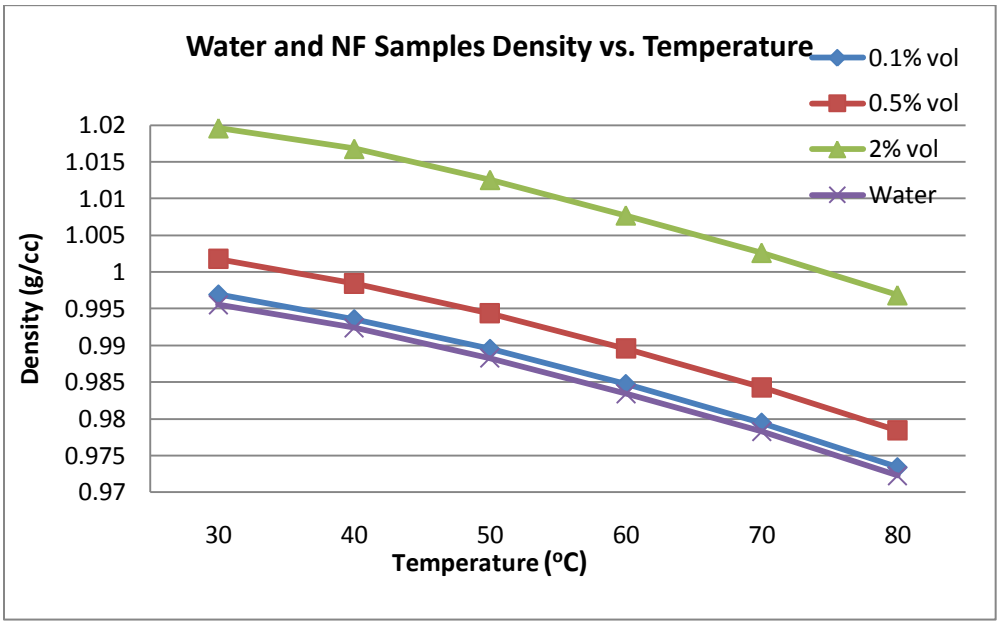

Figure 21. Density of nanofluids samples and water vs. temperature

6.3.3.2. Viscosity measurements

Viscosity can be measured with a falling ball viscometer which works based on how fast or slow a spherical ball moves into a fluid. Based on the time which lasts for the ball to run a specific distance

and its corresponding equation, one can measure the viscosity which is definitely dependent on the size and material of the ball and temperature of the fluid.

The correlation to find the theoretical viscosity is shown as follows:

The dynamic viscosity μ (in mPa.s) is calculated using the following equation:

$$\mu = K(\rho_1 - \rho_2).t \quad (41)$$

where:

- K = ball constant in mPa·s·cm^3/g·s
- ρ_1= density of the ball in g/cm^3
- ρ_2= density of the liquid to be measured at the measuring temperature in g/cm^3
- t = falling time of the ball in seconds.

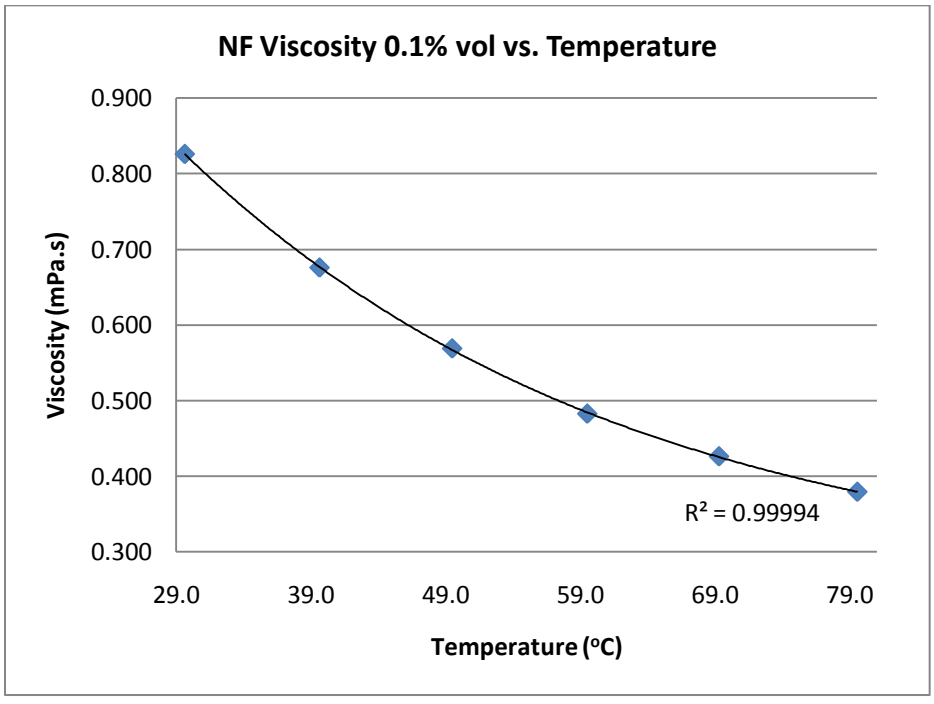

Figure 22. Nanofluid Viscosity of 0.1% vol sample vs. Temperature

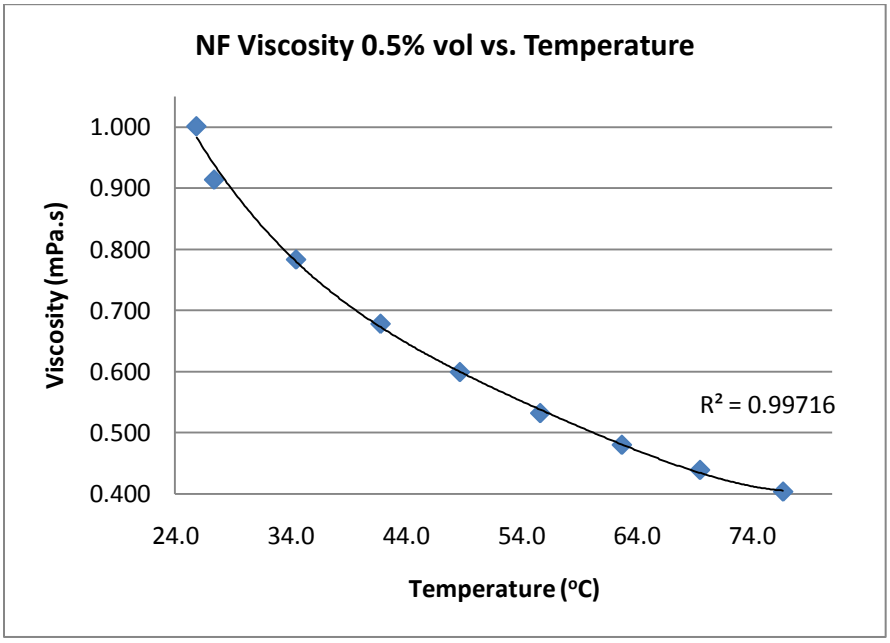

Figure 23. Nanofluid Viscosity of 0.5% vol sample vs. Temperature

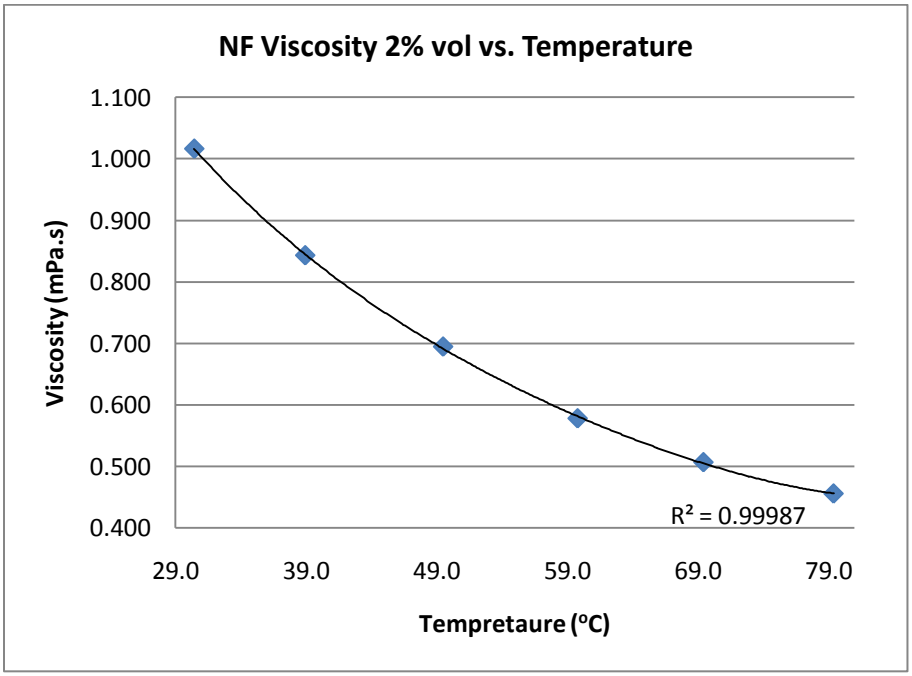

Figure 24. Nanofluid Viscosity of 2% vol sample vs. Temperature

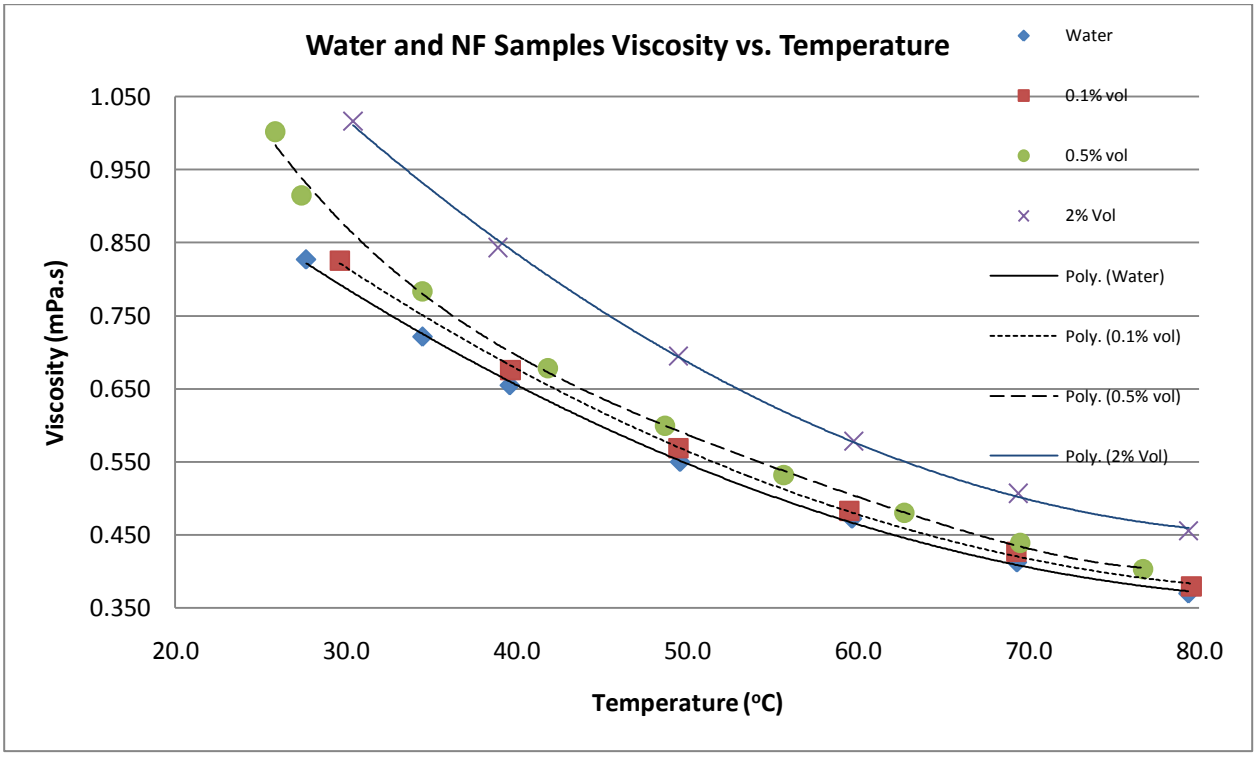

Figure 25. Viscosity of nanofluids samples and water vs. temperature

6.3.3.3. Thermal conductivity

The thermal conductivity measurements were done in the lab of chemistry department in Aalto University and since there was not temperature control over the experimental conditions, so the thermal conductivities are listed in the below table in their corresponding average fluid temperatures:

Table 4. Thermal conductivity of various samples in addition to water in their average temperature

Sample	k (W/mK)	AVG T (^{o}C)
0.1% vol	**0.620859**	**27.69493**
0.5% vol	**0.621427**	**28.47856**
2% vol	**0.623758**	**28.95561**
DI Water	**0.617422**	**29.14609**
DI Water	**0.615705**	**25.13152**

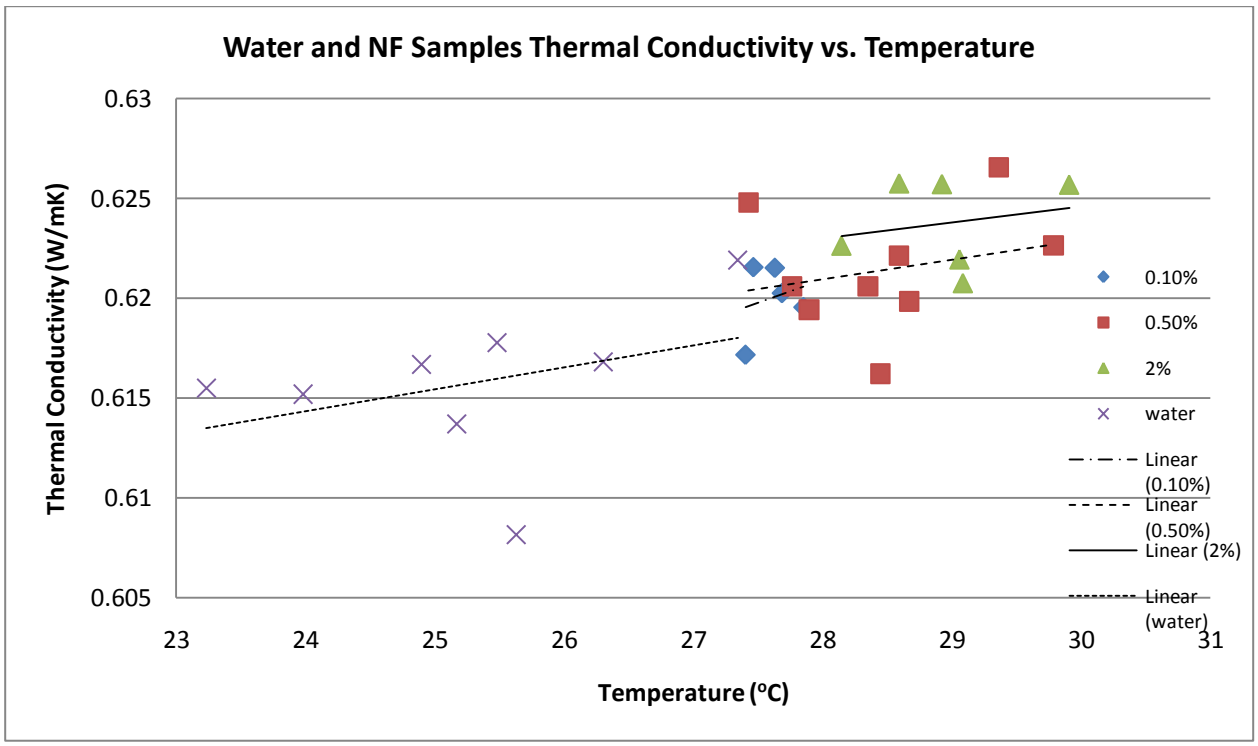

Figure 26. Thermal Conductivity of nanofluids samples and water vs. temperature

6.3.3.4. Specific heat

Specific heat results measured by DSC are as follows:

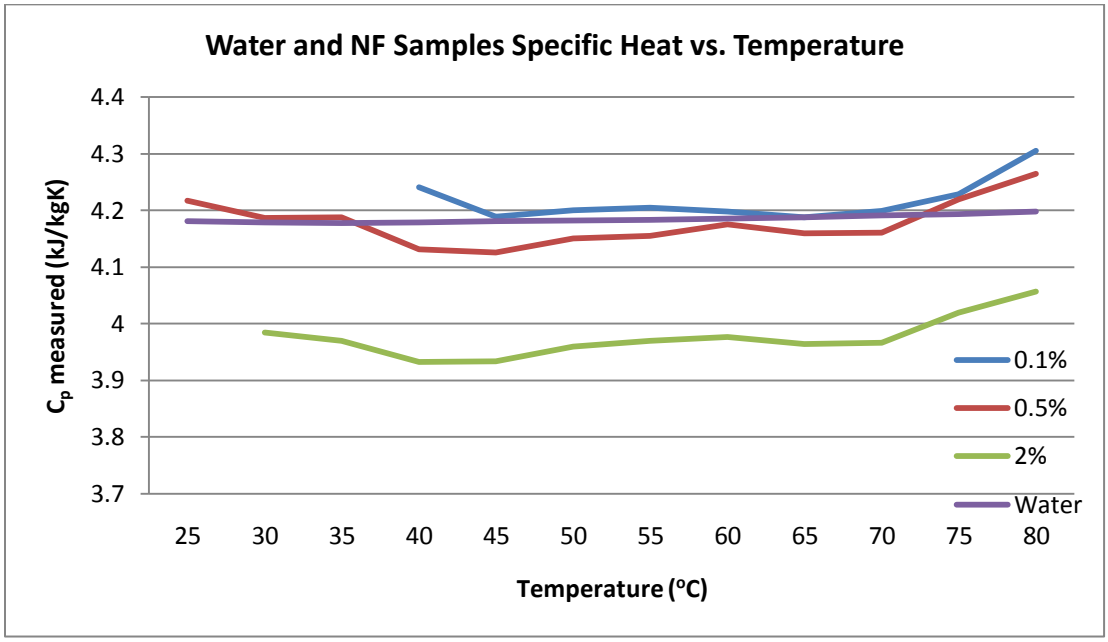

Figure 27. Specific heats of samples measured by DSC instrument vs. Temperature

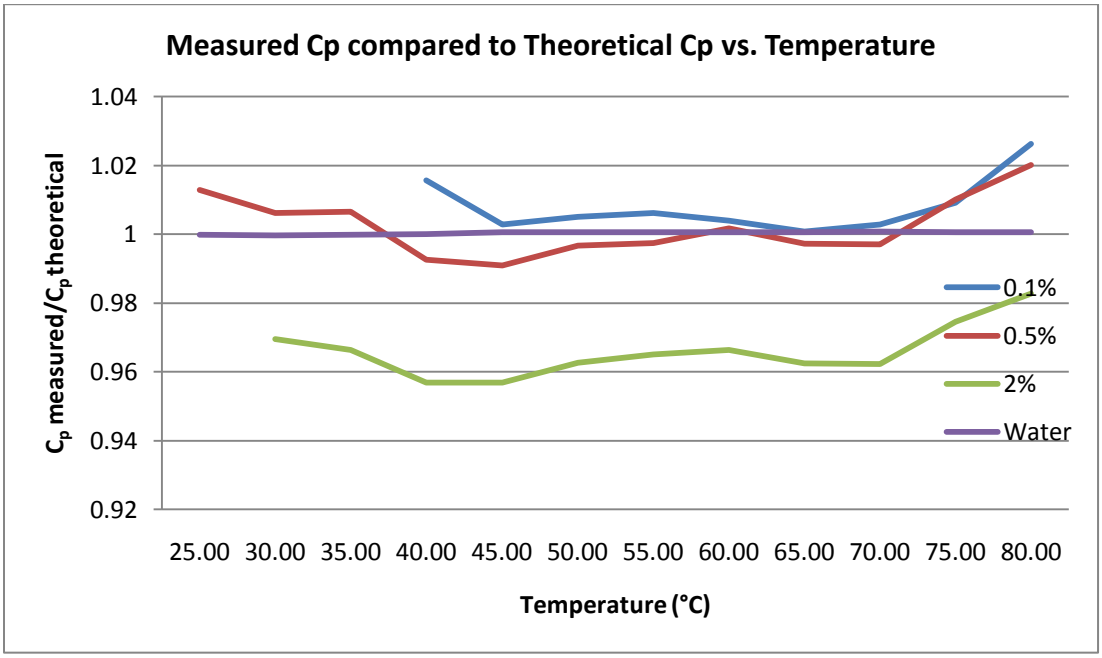

Figure 28. Ratio of Specific Heat measured to calculated vs. Temperature

Calculation of specific heat is done according to this formula:

$$C_{p,calc} = C_{p,meas,w} \times \varphi_w + C_{p,sil} \times \varphi_{sil} \quad (42)$$

where $C_{p,sil}$ is variable between 680-730 kJ/kg.K which is assumed to be the average 705 kJ/kg.K and volume fraction is 0.1 %, 0.5 % and 2 % for corresponding sample.

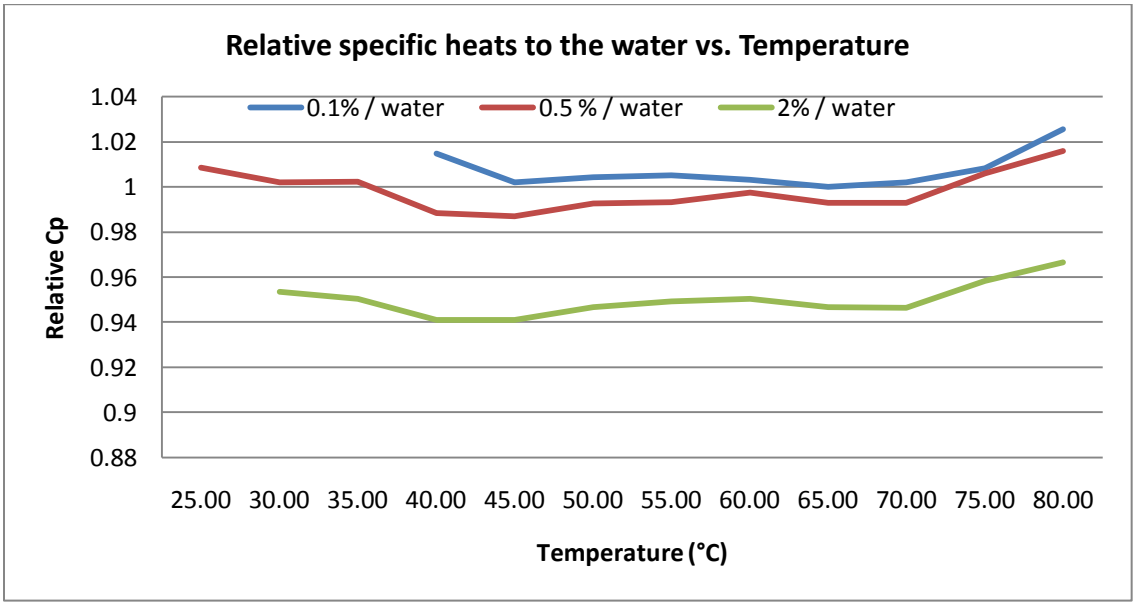

Figure 29. Relative Specific Heats (Ratio to water) vs. Temperature

6.4. Measurement of nanofluid characteristics

6.4.1. Size distribution

Size distribution has been outlined by three factors, Intensity, Number and Volume.

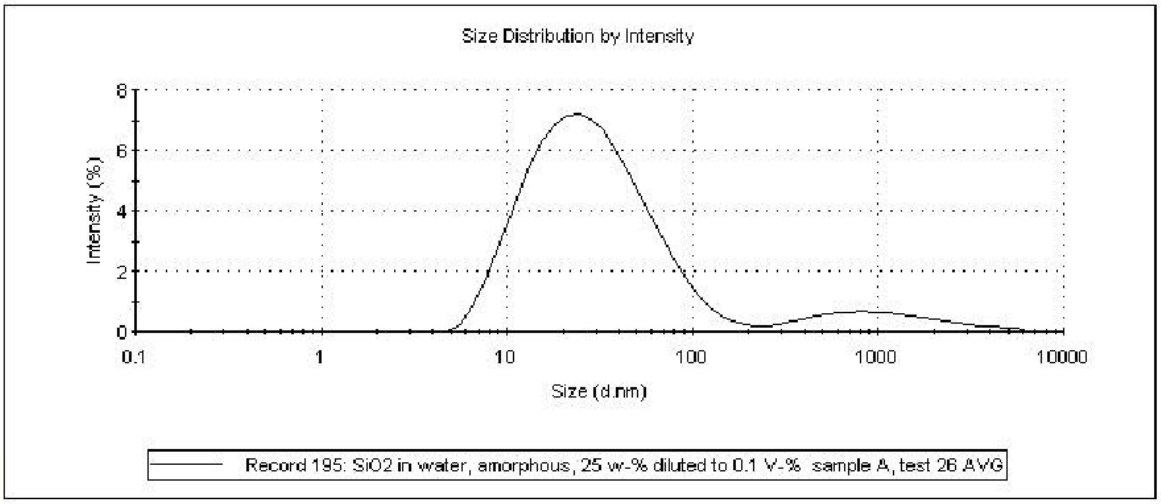

Figure 30. Intensity vs. Size for 0.1 V-% sample before HT experiment

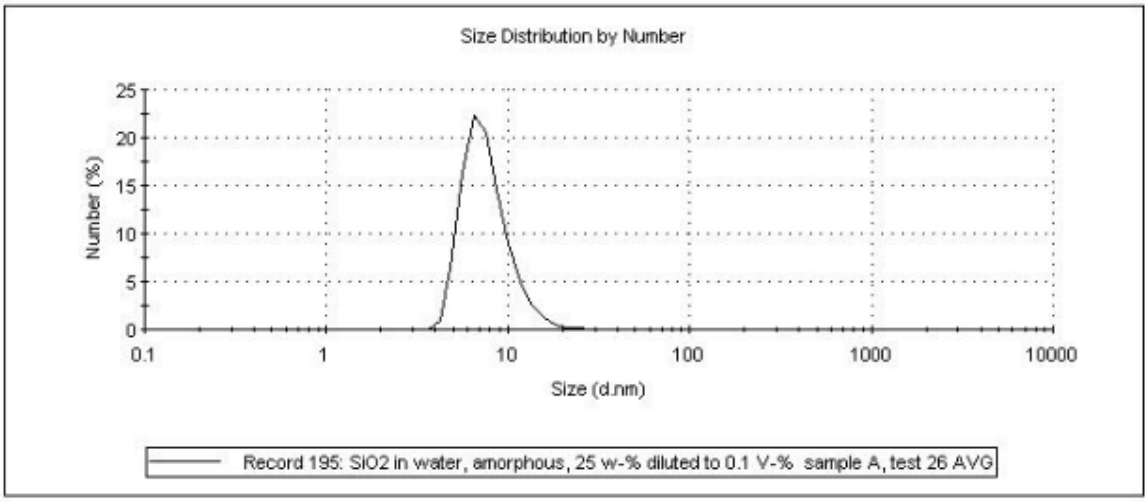

Figure 31. Number vs. Size for 0.1 V-% sample before HT experiment

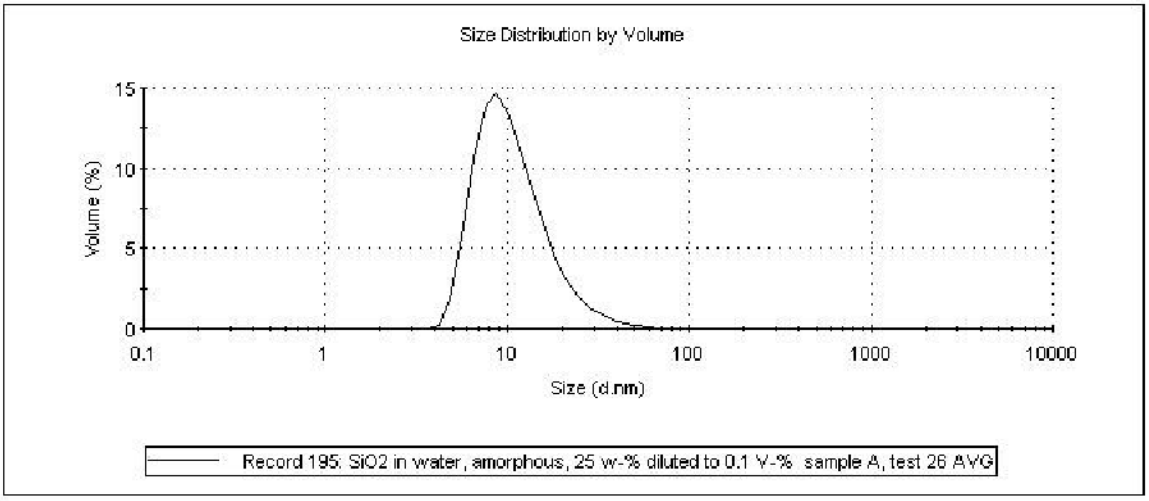

Figure 32. Volume vs. Size for 0.1 V-% sample before HT experiment

The samples used in the experiments should have been spherical silica nanofluids with diameter of 30 nm with 25% weight percent. As it was explained in detail in the previous chapters, samples should be analyzed right before and after the heat transfer measurements to make sure about their size and intensity.

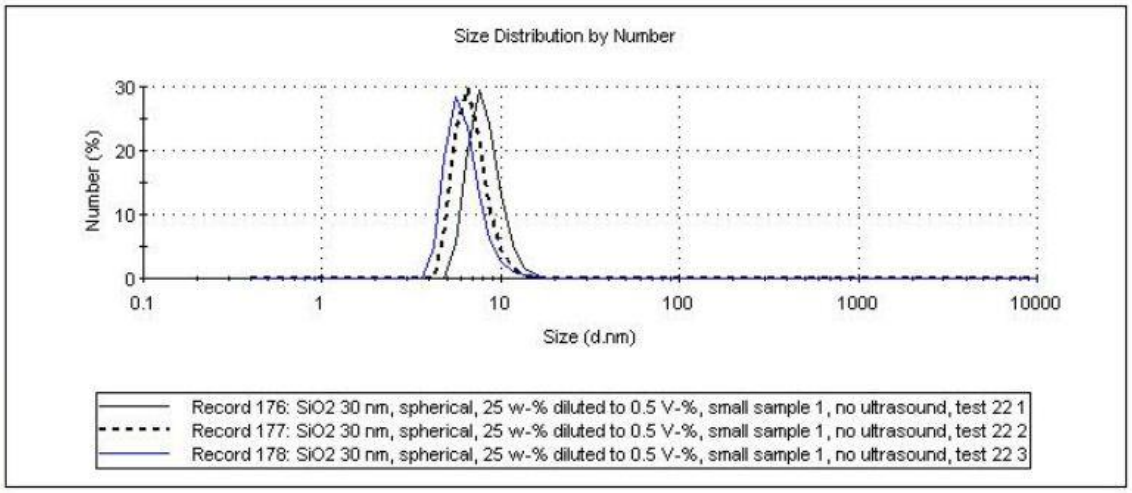

Figure 33. Volume vs. Size for 0.5 V-% sample before HT experiment

For other samples we have had similar figures before the heat transfer experiments.

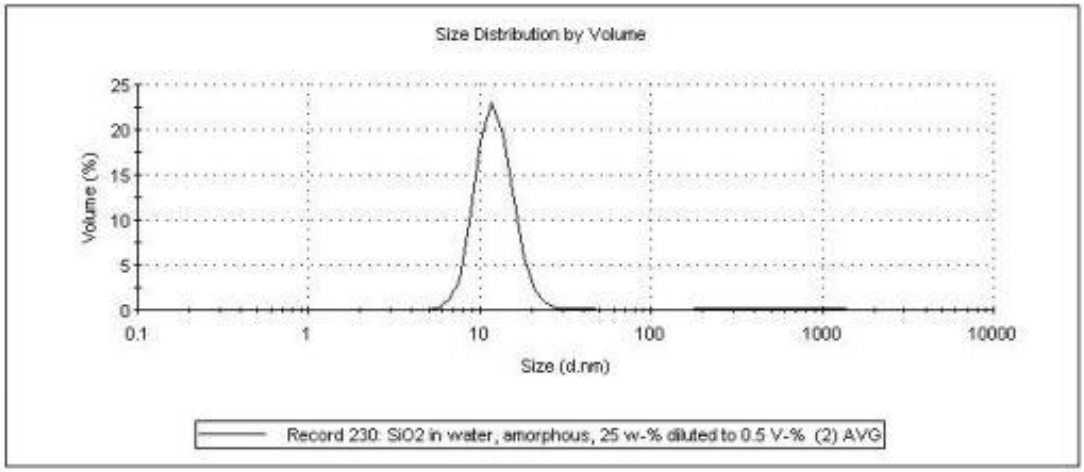

Figure 34. Volume vs. Size for 0.5 V-% sample after HT experiment

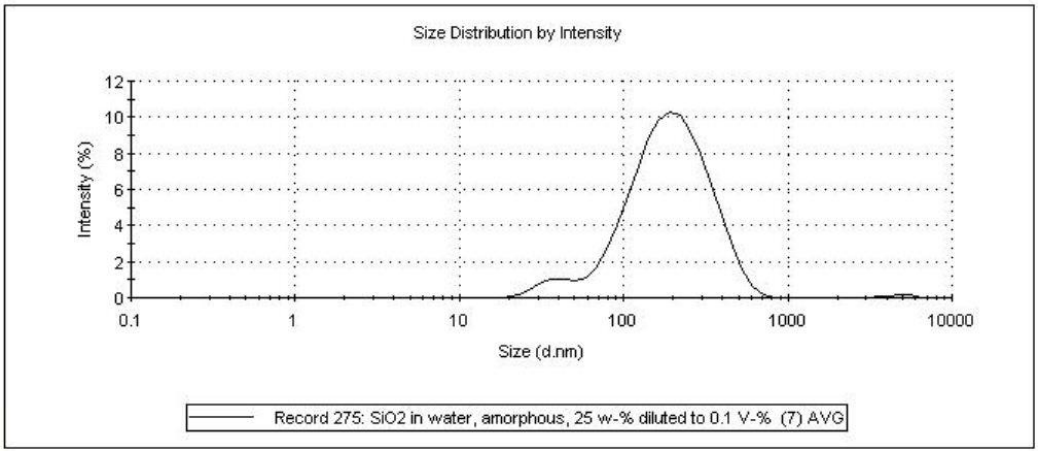

Figure 35. Volume vs. Size for 0.1 V-% sample after HT experiment where agglomeration occurred

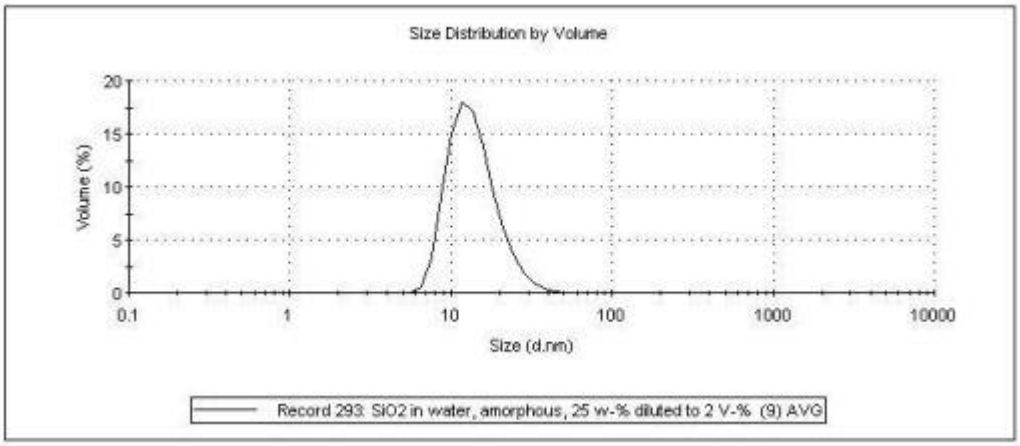

Figure 36. Volume vs. Size for 2 V-% sample after HT experiment with the average size of 14.2 nm

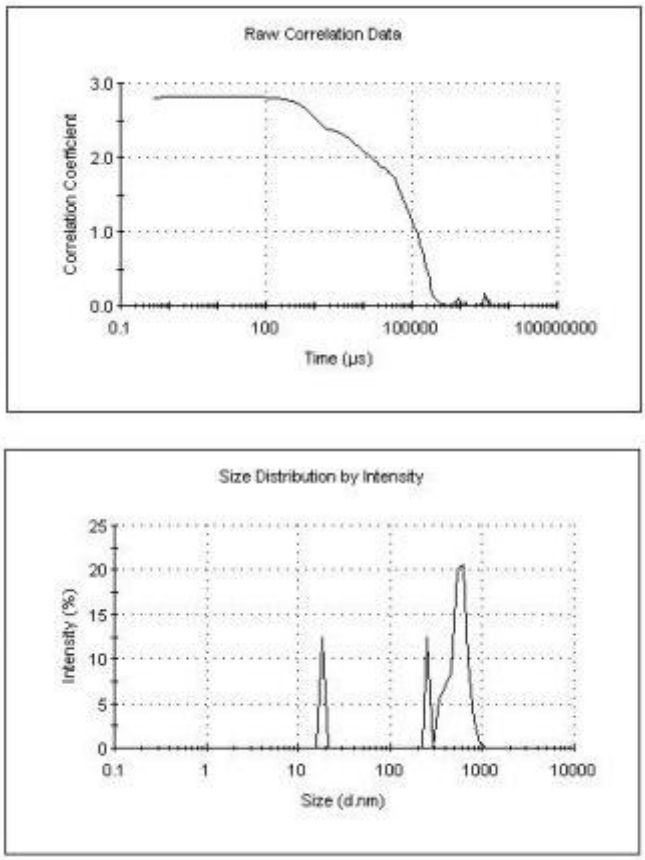

Figure 37. Intensity vs. Size for 0.1 V-% sample after HT experiment where agglomeration happened

Since the credibility of experimental results depends on the DLS results after the experiments, the experiment results in which agglomeration, aggregation or sedimentation happened are not credible. Fortunately due to the parallel measurements of 2-3 times for each sample, there are results for each sample that are credible.

7. RESULTS

In this section, the final heat transfer results will be presented and discussed.

7.1. Heat transfer

Heat transfer can be measured by two indicators, Nu number and heat transfer coefficient which will be presented as follows.

7.1.1. Nusselt number

In order to get the Nu we used four different correlations, as they were introduced in the previous chapters. Hausen and Sieder and Tate are used for laminar regime, while Gnielinski and Dittus Boelter (almost Dittus Boelter was not in the range for most of the data) are used for Turbulent flow. However, we cannot use either of these four for the Re in the range of 2300-3000 so for that range we have came up Nusselt number for boundary condition, while outer wall is insulated (R C et al. Armstrong, 1989):

$$\frac{Nu_i}{Nu_{tube}} = 0.86\left(\frac{d_i}{d_o}\right)^{-0.16} \quad (43)$$

These results have been accumulated by processing a lot of data from the measurements and converting their steady state data by averaging and then insert them into another Excel file with about 85 columns. So here, one can see only the final shot, without seeing the complexity behind this process.

7.1.1.1. Cooling Experiments

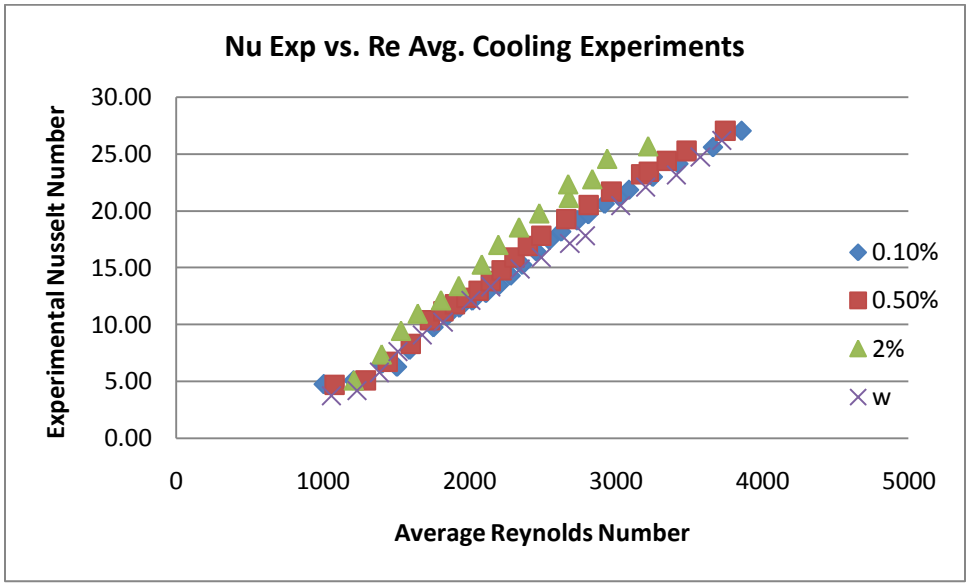

Figure 38. Experimental Nu vs. Re Average, Cooling experiments

7.1.1.2. Heating Experiments

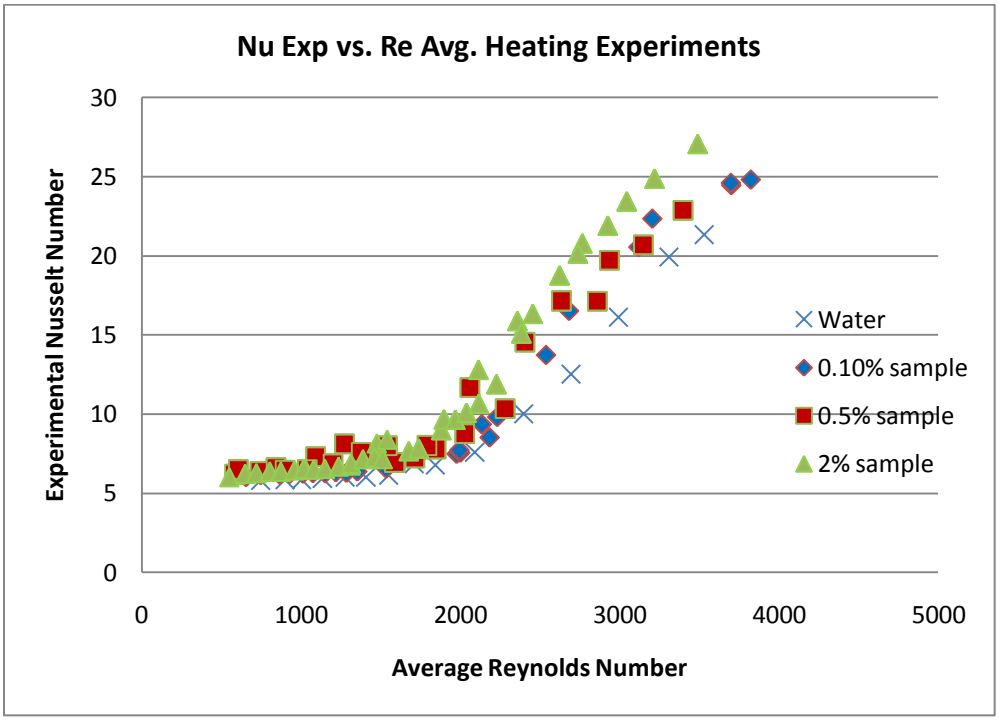

Figure 39. Experimental Nu vs. Re Average, Heating experiments

7.1.2. Convective heat transfer coefficient

Convective heat transfer coefficient for both cooling and heating sets of experiments is presented as follows.

7.1.2.1. Cooling Experiments

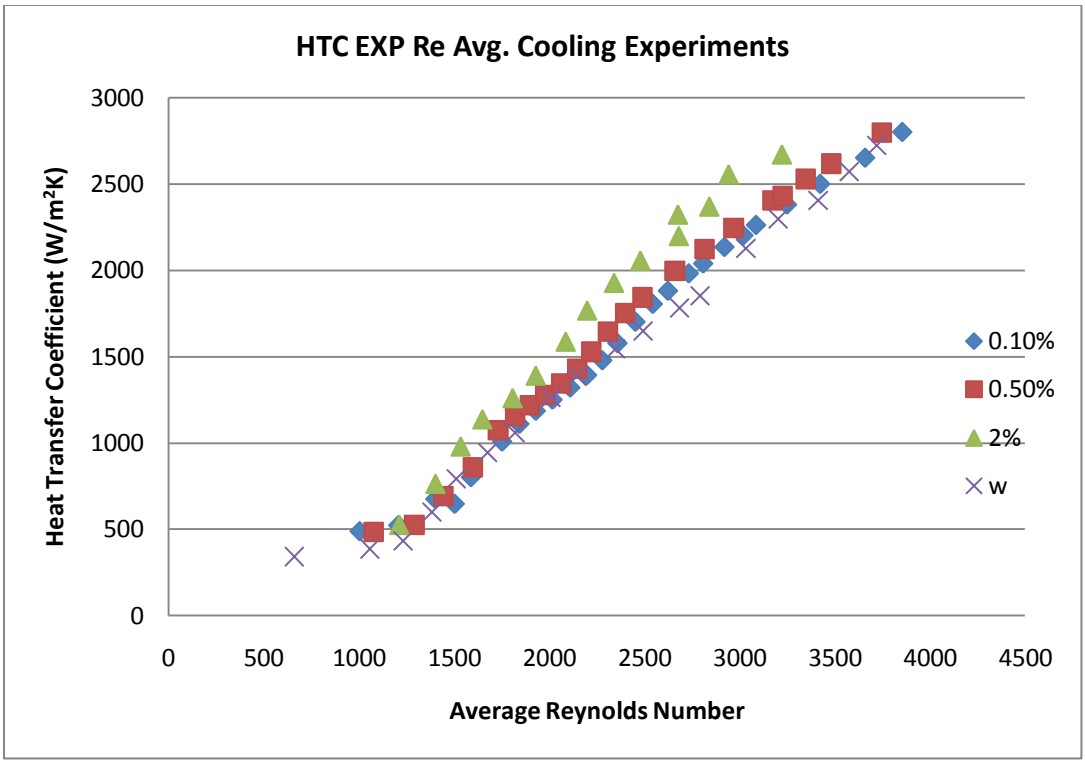

Figure 40. Heat Transfer Coefficient vs. Re Average, Cooling experiments

7.1.2.2. Heating Experiments

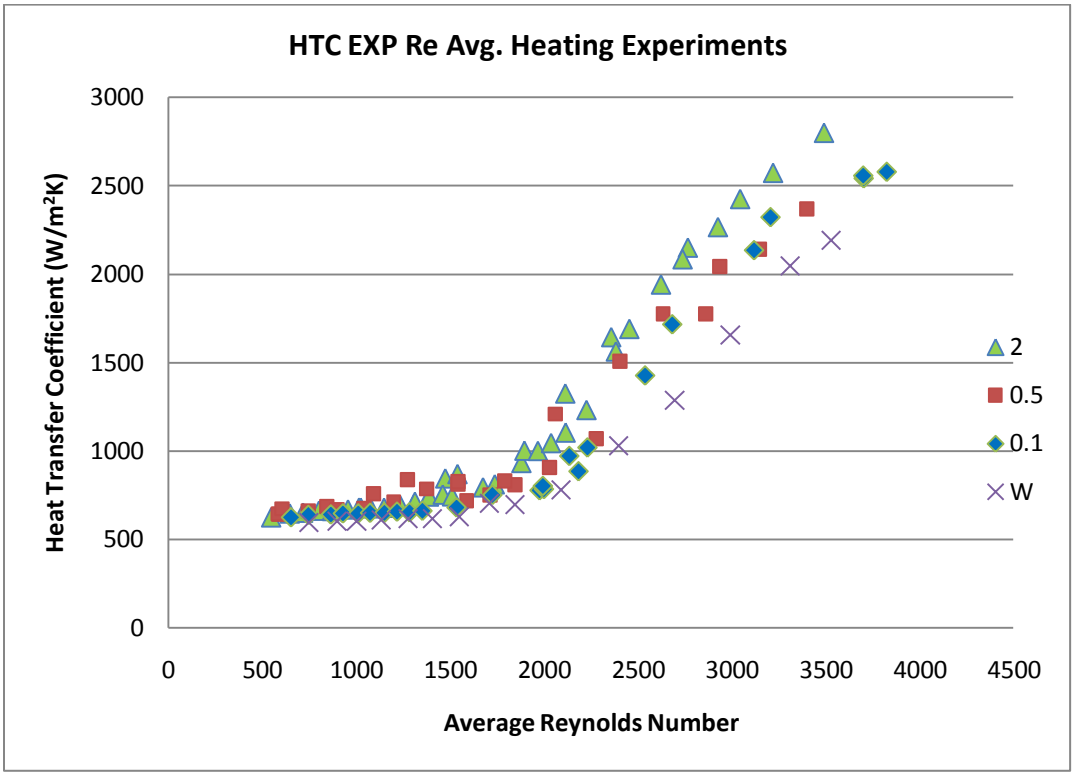

Figure 41. Heat Transfer Coefficient vs. Re Average, Heating experiments

7.2. Pressure drop and friction factor

The values of pressure drop from the measurements can give the friction factors.

$$\Delta P = \frac{fL\rho V^2}{2d} \qquad (44)$$

so based on the measurements, friction factor's trend is similar to the trend in Moody diagram. In turbulent regime, it goes as in Moody diagram while in laminar region the values are higher than that of Moody. In cooling experiments it seems that transition happens not at 2300 but a bit sooner in Re range of 1600-1800. For this, 0.1% results are a bit weird, but since we have no result for lower than Re=1220 we can only guess that its friction factor follows Moody's trend as other samples.

7.2.1. Cooling Experiments

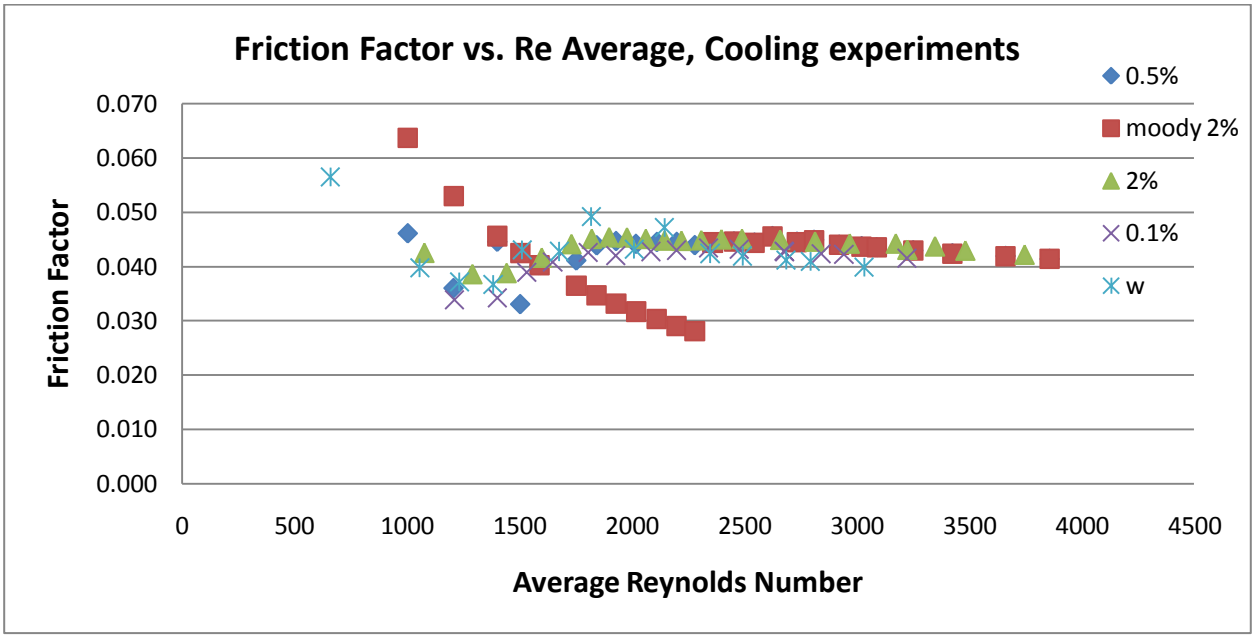

Figure 42. Friction Factor vs. Re Average, Cooling experiments including Moody

7.2.2. Heating Experiments

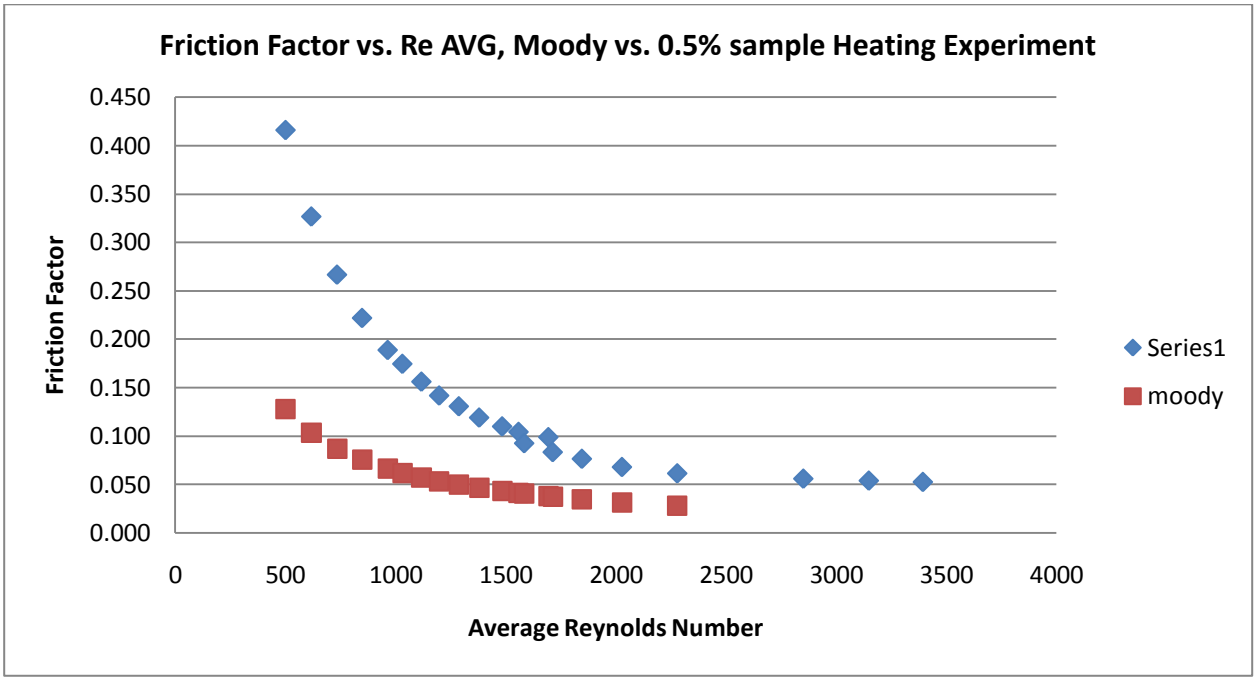

Figure 43. Friction Factor vs. Re Average, Heating experiment 0.5% sample

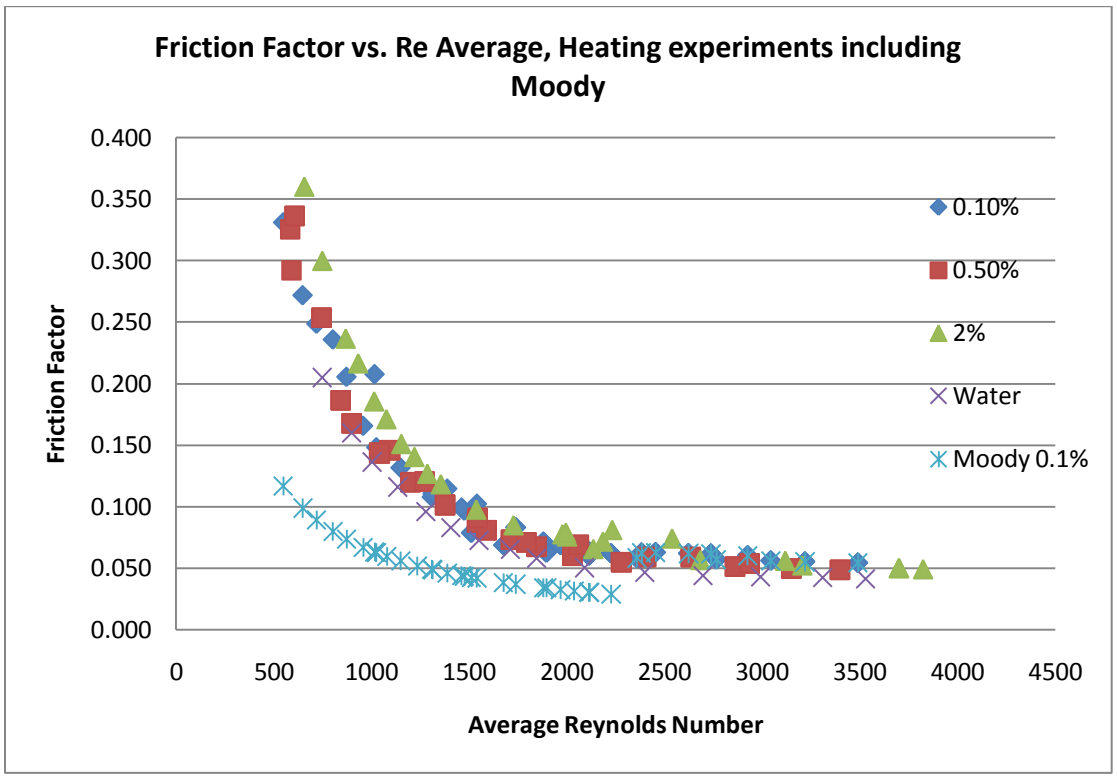

Figure 44. Friction Factor vs. Re Average, Heating experiments including Moody Chart

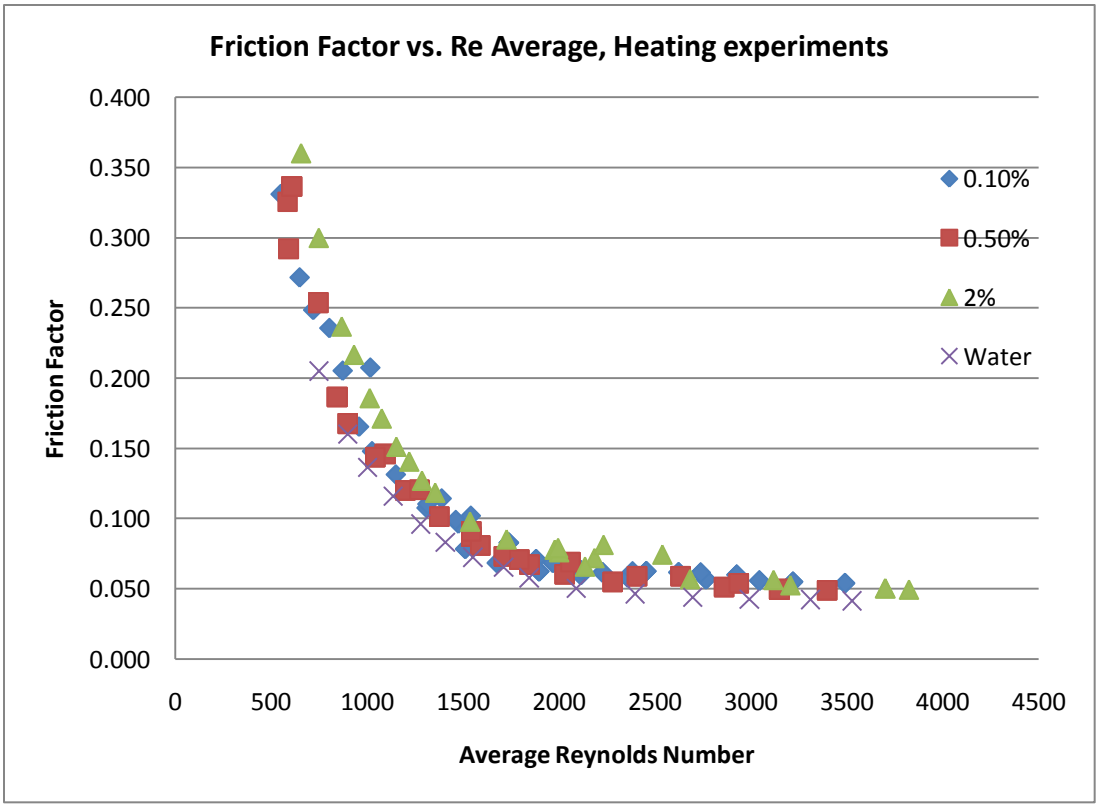

Figure 45. Friction Factor vs. Re Average, Heating experiments

7.3. Overall Efficiency

Overall efficiency has been calculated using the below formula as we explained the previous chapters.

$$\eta = \frac{\dot{Q}_{NF}}{P_{Pump\ ,NF}} \times \frac{P_{Pump\ ,W \to NF}}{\dot{Q}_{W \to NF}} \times 100 \qquad (45)$$

where we need to find the pumping power and heat transfer rate if we have had water as nanofluid. Since our measurements for water are in different Re and flow rates we need to find the trend of characteristics of water and then calculate NF properties based on that.

7.3.1. Cooling Experiments

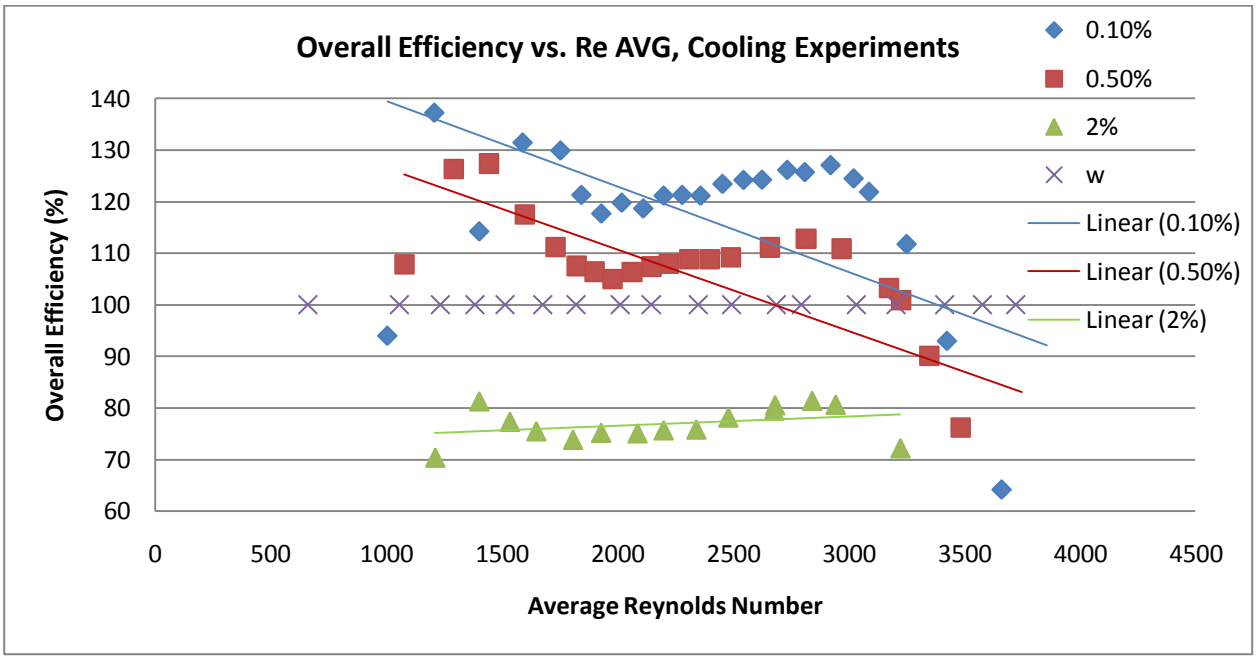

Figure 46. Overall Efficiency vs. Re Average, Cooling experiments

7.3.2. Heating Experiments

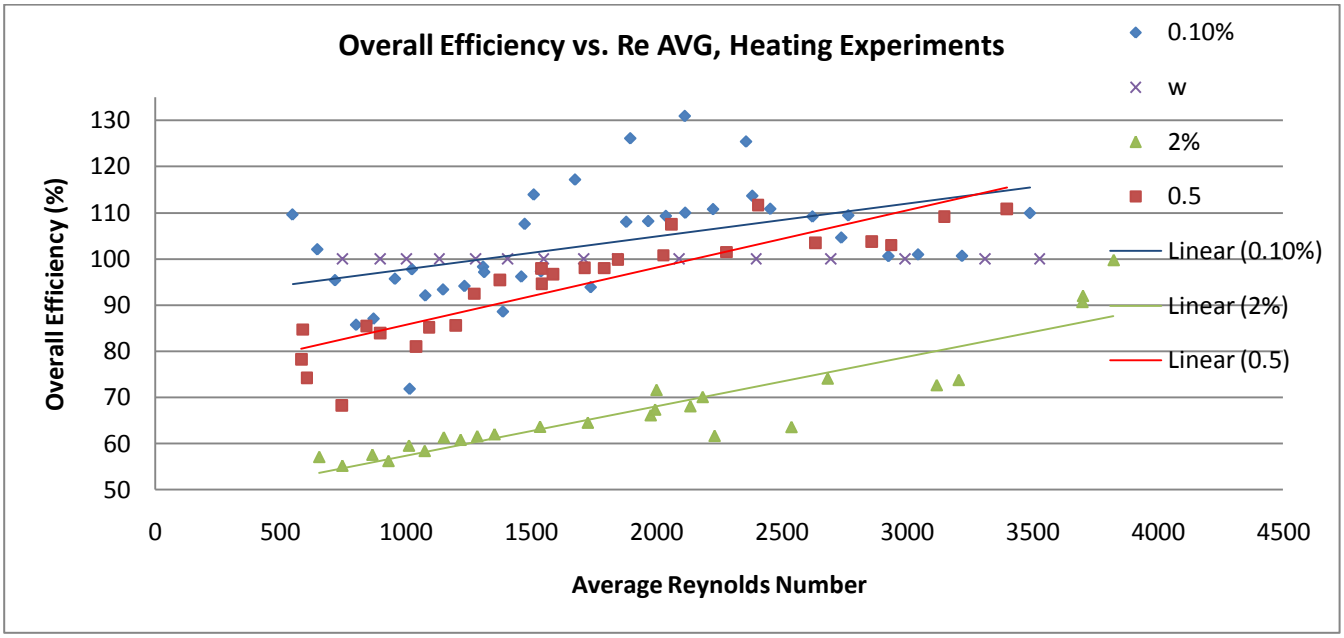

Figure 47. Overall Efficiency vs. Re Average, Heating experiments

Table 5. Average overall efficiency compared to water in heating and cooling experiments

Average Overall Efficiency, compared to that of water	Heating	Cooling
0.1%	**103%**	**116%**
0.5%	94%	**105%**
2%	68%	77%

So based on all of the results one can see that the sample with the volumetric nanoparticle concentration of 0.1% gives better overall efficiency both in cooling and heating. The next better results belong to 0.5% sample and finally 2% sample which although showed better heat transfer capability, will waste a lot more energy from the pumping point of view.

8. CONCLUSION

In this project, effect of volumetric concentration of silica nanoparticles in water as base fluid has been investigated in terms of heat transfer and pressure drop in the vertical concentric circular tube heat exchanger in a counterflow scheme in which water flows downward in the outer tube and nanofluid (NF) in 3 volume concentrations of 0.1% 0.5% and 2% flows upwards in the inner tube. All the necessary properties such as temperature of NF right before and after heat exchanger, its pressure drop within the test tube and flow speed and water properties such as temperature and flow speed have been measured in both cases of heating and cooling of the NF. The rest of properties of NF and water have been measured after the measurements such as thermal conductivity, density, viscosity and specific heat in order to find the Nu number and heat transfer coefficient. The main key of this research is to see how the properties will vary while heating and cooling alters the flow regime from turbulent Re numbers to laminar ones and vice versa within transition regime. Based on the results obtained, lower concentrations show better results than water in terms of heat transfer coefficient while a bit increase in pumping can be observed.

8.1. Limitations and Future Research

There were some limitations as the heater capacity for the maximum temperature of tank at the start of the experiments and also stabilization of the flow took long time. Various modifications to the experimental setup like changing the second heat exchanger after the main heat exchanger or replacing the pressurized air by pressurized CO2 made the experiment conditions inconsistent for comparison. For instance, by adding the new heat exchanger or Haake bath, the overall length of experimental cycle increased.

In addition, controlling the heating water temperature of the thermal bath for the heating experiment of nanofluids was a bit difficult because of the small capacity of the thermal bath and malfunctioning of its thermostat due to the high temperatures which leaded to consecutive turning off and on for the thermostat.

Agglomeration was observed on some samples before using them for the heat transfer experiment or

some of the samples after the experiment affected the duration of experiments and the credibility of the results. Fortunately, although about a bit more than the half of samples showed the signs of agglomeration and aggregation, our parallel measurements, usually between 3 to 4 different sets of experiments, were quite enough to make us do the rest of calculations. It should be mentioned that some of the results are attributed as agglomerated or aggregated because of their average particle size. However, there is inevitable dirt which consists of larger particles that has become loose from the heat transfer equipment, those particles should not affect the results because the samples were filtered after the measurements and the particle size of the agglomerated results are not as big as the dirt particles, but in the range of 50-100 nm.

The results as we expected prove the instability of flow in transition region and although the results were quite unstable, due to the highly changing of the flow type, higher HTC was observed.

Some of our results seem to be not completely according to the trend we expected. Those results could be due to the inconsistent conditions of experiment or inevitable errors in reading and calculating the data, especially when we had to assume nanofluid as water and follow water trends. For example, in few points we see that friction factor for lower concentration samples are bigger than that of higher concentration samples. However, the overall trend looks promising.

Friction factor calculations are hugely dependent on the pressure meter and as it is very sensitive, a small error in its measurement can yield a big error. Especially inevitable bubbling which happens after several hours can vary the pressure drop. The uncertainty seems to be high for pressure drop measurements although by neglecting few of the weird values, perhaps due to the errors, the trends are as expected from the theory so the friction factor results can almost be comparable with each other although not with the theoretical expectations.

There should be some errors 2-12% in the calculations pertaining to the overall efficiency, since we assigned the nanofluid characteristics to the water trend. So even, with this error margin, still 0.1% sample shows higher overall efficiency than that of water.

For the future research, this would be a good idea to compare 0.1%-vol silica nanofluids with 0.05%, 0.08%, 0.2% and 0.3%-vol to find the most optimum case. It is recommended that calibration of

pressure meter, after each measurement be carried out. It would be even better to make it calibrated within the same set of measurements because in some cases bubbles in the pressure meter were observed that may change the initial settings and can affect uncertainty to the results.

8.2. Summary

As one can see the best heat transfer performance of silica nanofluids in transitional flow, dispersed in pure water is observed in 0.1%-vol sample. According to what has been discussed in the introduction, there are plenty of applications for this medium to improve the heating efficiency like in any kind of heat exchanger from computer processors in data centers that are running 24/7, refrigerators as household or industrial usage, vehicle radiators, coolers and chillers, heat pumps, district heating tubes and on and on.

As this research predicts that equipping the fluids in heat exchangers with proper nanoparticles may increase the heating and cooling efficiency of appliances by 5-15% and this may lead to five main benefits from the environmental vantage point:

- One is decreasing the size of current heat exchangers by this ratio, so it may result in smaller car engines. So in this advantage, we may have lower dimensions for the current devices.
- The second advantage is that it can decrease the energy consumption since the fluid is stronger for instance in cooling fans for processors there might be lower fan power to cool down the same amount of heat.
- The third is that having the same size or energy can increase the life cycle of the same device so for instance, a heat exchanger can live few years more and it can decrease the replacement expenses as well as emissions to the soil, air and water.
- The fourth benefit is that usage of nanofluids can impose less emission to the environment due to the less usage of material for the same purpose. The resources on earth are not infinite and converting the raw materials to appliances that go out of use in a short time does not seem to be wise.
- The last but not least is to replace the harmful refrigerants like CFCs that can damage the Ozone layer with just adding nanoparticles to the conventional fluids like water and ethylene glycol.

REFERENCES

Bohne, D., Fischer, S. and Obermeier, E. (1984). Thermal, conductivity, density, viscosity, and Prandtl-numbers of ethylene glycol-water mixtures. *Berichte der Bunsengesellschaft für physikalische Chemie*, 88(8), pp.739-742

Çengel, Y. (2003). *Heat Transfer*. Boston: McGraw-Hill

Çengel, Y. (2007). *Heat and Mass Transfer*. Boston: McGraw-Hill

Çengel, Y. and Ghajar, A. (2011). *Heat and Mass Transfer*. New York: McGraw-Hill

Çengel, Y. and Cimbala, J. (2010). *Fluid Mechanics*. New Delhi, India: Tata McGraw Hill Education Private, p.325

Cianfrini, M., Corcione, M. and Quintino, A. (2011). Natural convection heat transfer of nanofluids in annular spaces between horizontal concentric cylinders. *Applied Thermal Engineering*, 31(17-18), pp.4055-4063

Dahneke, B. (1983). *Measurement of suspended particles by quasi-elastic light scattering*. New York: Wiley

Ding, Y., Chen, H., He, Y., Lapkin, A., Yeganeh, M., Šiller, L. and Butenko, Y. (2007). Forced convective heat transfer of nanofluids. *Advanced Powder Technology*, 18(6), pp.813-824

Einstein, A. (1905). Über die von der molekularkinetischen Theorie der Wärme geforderte Bewegung von in ruhenden Flüssigkeiten suspendierten Teilchen. *Ann. Phys.*, 322(8), pp.549-560

Ford, B. (1992). Brownian movement in clarkia pollen: a reprise of the first observations. *Microscope-London Then Chicago-*, 40, p.235

Guo, S., Li, Y., Jiang, J. and Xie, H. (2010). Nanofluids Containing γ-Fe2O3 Nanoparticles and Their Heat Transfer Enhancements. *Nanoscale Res Lett*, 5(7), pp.1222-1227

Jung, J. and Yoo, J. (2009). Thermal conductivity enhancement of nanofluids in conjunction with electrical double layer (EDL). *International Journal of Heat and Mass Transfer*, 52(1-2), pp.525-528.

K R, S., Nair, A., K M, V., T R, S. and Nair, S. (2014). An overview of recent nanofluid research. *International Research Journal of Pharmacy*, 5(4), pp.239-243.

Kumaresan, V., Mohaideen Abdul Khader, S., Karthikeyan, S. and Velraj, R. (2013). Convective heat transfer characteristics of CNT nanofluids in a tubular heat exchanger of various lengths for energy efficient cooling/heating system. *International Journal of Heat and Mass Transfer*, 60, pp.413-421

Liao, J., Zhang, Y., Yu, W., Xu, L., Ge, C., Liu, J. and Gu, N. (2003). Linear aggregation of gold nanoparticles in ethanol. *Colloids and Surfaces: Physicochemical and Engineering Aspects*, 223(1-3), pp.177-183.

Lin, Y., Wu, S., Tseng, C., Hung, Y., Chang, C. and Mou, C. (2009). Synthesis of hollow silica nanospheres with a microemulsion as the template. *Chem. Commun.*, (24), p.3542

Maïga, S., Palm, S., Nguyen, C., Roy, G. and Galanis, N. (2005). Heat transfer enhancement by using nanofluids in forced convection flows. *International Journal of Heat and Fluid Flow*, 26(4), pp.530-546.

Meibodi, M., Vafaie-Sefti, M., Rashidi, A., Amrollahi, A., Tabasi, M. and Kalal, H. (2010). Simple model for thermal conductivity of nanofluids using resistance model approach. *International Communications in Heat and Mass Transfer*, 37(5), pp.555-559.

Meriläinen, A., Seppälä, A., Saari, K., Seitsonen, J., Ruokolainen, J., Puisto, S., Rostedt, N. and Ala-Nissila, T. (2013). Influence of particle size and shape on turbulent heat transfer characteristics and pressure losses in water-based nanofluids. *International Journal of Heat and Mass Transfer*, 61, pp.439-448

Moody, L. (1944). Friction factors for pipe flow. *Trans. ASME*, 66(8), pp.671-684

Murashov, V. and Howard, J. (2011). *Nanotechnology Standards*. New York: Springer

Pecora, R. (1985). *Dynamic light scattering*. New York: Plenum Press

R C et al. Armstrong. (1989). Fluid Mechanics and Heat Transfer Hardcover. *Hemisphere Publishing Corporation*

Raithby, G. and Hollands, K. (1975). A General Method of Obtaining Approximate Solutions to Laminar and Turbulent Free Convection Problems. *Advances in Heat Transfer*, pp.265-315

Thomas, J. (1987). The determination of log normal particle size distributions by dynamic light scattering. *Journal of Colloid and Interface Science*, 117(1), pp.187-192.

Thomas, L. (2003). Making accurate DSC and MDSC® specific heat capacity measurements with the Q1000 Tzero™ DSC. *TA Bulletin TA310.TA Instruments, New Castle*, (2&id)

Tscharnuter, W. (2006). Photon Correlation Spectroscopy in Particle Sizing. *Applications, Theory and Instrumentation*

Tuchinsky, P. (1976). Poiseuille's law. *Modules in applied mathematics-Cornell University*, 68, pp.1-18

Wang, C., Gao, P., Tan, S. and Wang, Z. (2013). Forced convection heat transfer and flow characteristics in laminar to turbulent transition region in rectangular channel. *Experimental Thermal and Fluid Science*, 44, pp.490-497

Washington, C. (1992). *Particle size analysis in pharmaceutics and other industries*. New York: E. Horwood

Watkinson, A., Bunge, A., Hadgraft, J. and Lane, M. (2013). Nanoparticles do not penetrate human

skin—a theoretical perspective. *Pharm Res*, 30(8), pp.1943-1946.

White, F. (2003). *Fluid Mechanics*. Boston: McGraw-Hill

White, F. (2006). *Viscous Fluid Flow*. New York, NY: McGraw-Hill Higher Education

Xie, H., Li, Y. and Yu, W. (2010). Intriguingly high convective heat transfer enhancement of nanofluid coolants in laminar flows. *Physics Letters A*, 374(25), pp.2566-2568

Xu, R. (2001). *Particle characterization: light scattering methods*. Dordrecht [u.a.]: Kluwer.

Americanelements.com, (2014). Silicon Dioxide SiO2 | AMERICAN ELEMENTS ® Supplier & Info. [online] Available at: http://www.americanelements.com/siox.html [Accessed 10 Dec. 2014]

Andersonmaterials.com, (2014). Differential Scanning Calorimetry (DSC) Thermal Analysis | Anderson Materials Evaluation, Inc.. [online] Available at: http://www.andersonmaterials.com/dsc.html [Accessed 12 Dec. 2014]

Azom.com, (2014). Properties: Silica - Silicon Dioxide (SiO2). [online] Available at: http://www.azom.com/properties.aspx?ArticleID=1114 [Accessed 12 Dec. 2014]

Bhaskar Kumar IIT Roorkee. (2011). Laminar, Transitional and Turbulent Flows [online] Available at: http://www.leb.eei.uni-erlangen.de/winterakademie/2011/report/content/course01/pdf/0103.pdf [Accessed 10 Dec. 2014]

Biomechanics: motion, flow, stress, and growth. (1990). *Choice Reviews Online*, 28(04), pp.28-2130-28-2130

Biophysics.bioc.cam.ac.uk, (2014). *Biophysics Facility*. [online] Available at: http://www.biophysics.bioc.cam.ac.uk/ [Accessed 12 Dec. 2014]

Dynamic light scattering. Common terms defined, (2011) *Malvern Instruments Limited*

Engineeringtoolbox.com, (2014). Laminar, Transitional or Turbulent Flow. [online] Available at: http://www.engineeringtoolbox.com/laminar-transitional-turbulent-flow-d_577.html [Accessed 10 Dec. 2014]

Hackley, V. and Clogston, J. (2010). Measuring the Hydrodynamic Size of Nanoparticles in Aqueous Media Using Batch-Mode Dynamic Light Scattering. *Methods in Molecular Biology*, pp.35-52

Horiba.com, (2014). Z-Average Particle Size: An Explanation - HORIBA. [online] Available at: http://www.horiba.com/scientific/products/particle-characterization/education/sz-100/particle-size-by-dynamic-light-scattering-resources/what-is-z-average/ [Accessed 12 Dec. 2014]

Hydrometer, [online] Available at: http://beer.wikia.com/wiki/Hydrometer [Accessed 12 Dec. 2014]

Physicsworld.com (2004). Turbulent transition for fluid [online] Available at: http://physicsworld.com/cws/article/print/2004/dec/01/turbulent-transition-for-fluids [Accessed 10 Dec. 2014]

Z. Warhaft. (1997). An Introduction to Engineering, Cambridge University, [online] Available at: https://www.princeton.edu/~asmits/Bicycle_web/transition.html [Accessed 10 Dec. 2014]

Zeta-reader.com, (2014). Welcome to Zeta Potential instruments, inc.. [online] Available at: http://www.zeta-reader.com/pages/overview.html [Accessed 12 Dec. 2014]

APPENDIX

Appendix I. Degassing the system

1. At first, all the valves should be closed and system is off.
2. If we use only the turbulent pump, open two valves of turbulent pump, otherwise, valves of laminar pump should be opened, as well. It's better to use both pumps for degassing the system since they have more power together.
3. Close the second black valve (on top), which is located after the T shape when the flow passes.
4. Start the pump(s) with the highest speed.
5. Open the bubble removal valve, (highest valve) and of course one should hold a bottle or beaker below the tube to collect the nanofluid.
6. Wait and collect as much nanofluid as there remains some fluid in the reservoir for pump to suck. Repeat this step over and over again until you make sure that there is no bubble coming out of the small hose.
7. There are two other points for degassing the system, such as at the drainage tube. The procedure is similar to what described above (the red hose which is connected to laminar pump can be used to degas the system, as well).
8. Flow meter should be degassed with opening its two screws and closing them.
   (It should be mentioned that flow meter has been put inside a metallic cage to remove the induction of electromagnetic effects which can alter the measured data and cause error).

Appendix II. Draining the nanofluid

1. At first, all the valves should be closed and system is off.
2. If we use only the turbulent pump, open two valves of turbulent pump, otherwise, valves of laminar pump should be opened, as well. It's better to use both pumps for draining the system since they have more powers together.
3. Close one of black valves (on top), the one located before the T shape when flow passes.
4. Start the pump(s) with the highest speed.
5. Open one of the drainage valves (red valve). There are two, one with the red tube connected to that and one with the blue tube connected to that. So, blue one should be opened and of course one should hold a bottle or beaker below the tube to collect the nanofluid (not to waste it). Then, there are two black valves which the right one should be closed. (the one that flow reaches later) If we use only the turbulent pump, we may not use the other draining tube (connected to red tube) as it brings the laminar pump into the cycle which is not supposed to do.
6. Wait and collect as much nanofluid until you feel that the pump is sucking air.
7. Then, shut off the pump quickly.
8. Now, most of the nanofluid has been drained out of the pipes, except for some small amount that requires compressed air or pressurized CO_2.
9. So, one needs to open the left valve on top (with the key) which is connected to pressurized CO_2 or compressed air vessels.
10. Put the metal plate with the load over the reservoir lid to seal the system and put the bottle below the blue pipe.
11. Open a little bit the pressurized CO_2 valve and watch nanofluid exiting. One must make sure not to increase the pressure which can disturb the fittings and joints.
12. When you make sure that no fluid is exiting, close the pressurized CO_2 valve.
13. Close the other upper black valve and close the open one. Close the open black valve which is connected to the blue tube hose and open the closed black one.
14. Repeat the step 11.
15. There should be no fluid after all.
16. Close the left valve (for air or CO_2) with the key on top and close the red valve. (for drainage) Open two black valves, one on top and one at the bottom.